PRELIMINARY THERMAL MODELING OF HI-STORM 100 STORAGE MODULES AT DIABLO CANYON POWER PLANT ISFSI

Fuel Cycle Research & Development

Prepared for
U.S. Department of Energy
Used Fuel Disposition Campaign

JM Cuta
HE Adkins
April 17, 2014
FCRD-UFD-2014-000505
PNNL-23298

Reviewed by:

PNNL Project Manager

Signature on file

_____

Brady Hanson

SUMMARY

This report fulfills the M4 milestone M4FT-14PN0810037.

Thermal analysis is being undertaken at Pacific Northwest National Laboratory (PNNL) in support of inspections of selected storage modules at various locations around the United States, as part of the Used Fuel Disposition Campaign of the U.S. Department of Energy, Office of Nuclear Energy (DOE-NE) Fuel Cycle Research and Development. This report documents pre-inspection predictions of temperatures for two modules at the Diablo Canyon Power Plant ISFSI identified as candidates for inspection. These are HI-STORM 100 modules of a site-specific design for storing PWR 17x17 fuel in MPC-32 canisters.

The temperature predictions reported in this document were obtained with detailed COBRA-SFS models of these storage systems, with the following boundary conditions and assumptions.

- storage module overpack configuration based on FSAR documentation of HI-STORM100S-218, Version B; due to unavailability of site-specific design data for Diablo Canyon ISFSI modules
- Individual assembly and total decay heat loadings for each canister, based on at-loading values provided by PG&E, "aged" to time of inspection using ORIGEN modeling
    - Special Note: there is an inherent conservatism of unquantified magnitude – informally estimated as up to approximately 20% -- in the utility-supplied values for at-loading assembly decay heat values
- Axial decay heat distributions based on a bounding generic profile for PWR fuel.
- Axial location of beginning of fuel assumed same as WE 17x17 OFA fuel, due to unavailability of specific data for WE17x17 STD and WE 17x17 Vantage 5 fuel designs
- Ambient conditions of still air at 50°F (10°C) assumed for base-case evaluations
    - Wind conditions at the Diablo Canyon site are unquantified, due to unavailability of site meteorological data
    - additional still-air evaluations performed at 70°F (21°C), 60°F (16°C), and 40°F (4°C), to cover a range of possible conditions at the time of the inspection. (Calculations were also performed at 80°F (27°C), for comparison with design basis assumptions.)

All calculations are for steady-state conditions, on the assumption that the surfaces of the module that are accessible for temperature measurements during the inspection will tend to follow ambient temperature changes relatively closely.

Comparisons to the results of the inspections, and post-inspection evaluations of temperature measurements obtained in the specific modules, will be documented in a separate follow-on report, to be issued in a timely manner after the inspection has been performed. Due to a number of delays in the document review process, this pre-inspection report is being published some time after the date of the inspections, which occurred in January 2014. However, the calculations and pre-inspection analysis reports work completed in November 2013, nearly two months prior to the inspections.

ACKNOWLEGMENTS

Holtec International generously allowed access to the FSAR for the HI-STORM 100 System, making possible construction of accurate and complete models of the HI-STORM100 Version B module, used as a 'stand in' for the site-specific modules at the Diablo Canyon ISFSI, for which information was unavailable. Special thanks are owed to Keith Waldrop of EPRI and Lawrence Pulley of PG&E, for supplying assembly loading data for the canisters selected as candidates for the inspection.

ACRONYMS AND ABBREVIATIONS

CFD	computational fluid dynamics
DOE	U.S. Department of Energy
DOE-NE	U. S. Department of Energy Office of Nuclear Energy
DSC	dry shielded canister
EPRI	Electric Power Research Institute
FEA	finite element analysis
ISFSI	independent spent fuel storage installation
MPC	multi-purpose canister
NCDC	National Climatic Data Center
NOAA	National Oceanic and Atmospheric Administration
ORNL	Oak Ridge National Laboratory
PGE	Pacific Gas and Electric Company (owner/operator of Diablo Canyon power plant and ISFSI)
PNNL	Pacific Northwest National Laboratory
PWR	Pressurized Water Reactor

CONTENTS

FIGURES

TABLES

PRELIMINARY THERMAL MODELING OF HI-STORM 100 STORAGE MODULES AT DIABLO CANYON POWER PLANT ISFSI

1.0 INTRODUCTION

As part of the Used Fuel Disposition Campaign of the U.S. Department of Energy, Office of Nuclear Energy (DOE-NE) Fuel Cycle Research and Development, a consortium of national laboratories[1] and industry[2] are performing inspections and temperature measurements of selected storage modules at various locations around the United States. In June 2012, inspections were performed on two horizontal storage modules in the Calvert Cliffs Nuclear Power Station's Independent Spent Fuel Storage Installation (ISFSI). Inspections were performed in November 2013 at the Hope Creek Nuclear Generating Station ISFSI, and in January 2014 at the Diablo Canyon Nuclear Power Station ISFSI. Thermal analysis in support of these inspections is being undertaken at Pacific Northwest National Laboratory (PNNL). Pre-inspection and post-inspection evaluations for the modules examined at Calvert Cliffs were performed using a detailed computational fluid dynamics (CFD) model of the storage module and the dry shielded canister (DSC) contained within it, using the STAR-CCM+ package. The results of these evaluations included temperature predictions in actual storage conditions for the module, DSC, and DSC contents, with preliminary estimates of fuel cladding temperatures (Suffield et al. 2012).

A similar effort is under way in support of the inspections at the Hope Creek Nuclear Generating Station ISFSI and at the Diablo Canyon Power Plant ISFSI. The Hope Creek site utilizes the HI-STORM 100S-218 Version B vertical storage system developed by Holtec International. The Diablo Canyon ISFSI utilizes a site-specific design in the HI-STORM 100 series, but no information was available on this design for the pre-inspection thermal analysis. Therefore, the design of the Hope Creek module overpack was used as a 'stand in' for the site-specific Diablo Canyon module geomtery. It is anticipated that the needed information on the site-specific geometry will be provided prior to final post-inspection evaluations of the data gathered at this site.

The basic feature of a HI-STORM 100 system, regardless of the specific configuration, consists of a helium-pressurized stainless steel canister that is loaded into a vertical steel-lined concrete overpack. The spent fuel is contained within the sealed canister, and the basket internal design varies with the type of fuel to be stored, with three main configurations available for PWR fuel and two for BWR fuel. Thermal models have been developed for the modules to be inspected at Hope Creek and Diablo Canyon, using COBRA-SFS (Michener et al. 1995), a code developed by PNNL for thermal-hydraulic analyses of multi-assembly spent fuel storage and transportation

[1] Pacific Northwest National Laboratory, Oak Ridge National Laboratory, Sandia National Laboratories, and Idaho National Laboratory

[2] Electric Power Research Institute, TN/AREVA, Holtec International, PSEG Nuclear LLC (owner of Hope Creek Nuclear Generating Station), Constellation Energy (Owner of Calvert Cliffs Nuclear Power Station), and Pacific Gas and Electric Corporation (owner of Diablo Canyon Power Plant).

systems. Pre-inspection predictions of temperatures for the selected modules in the ISFSI at Hope Creek were published earlier (Cuta and Adkins, 2013). The current document presents similar pre-inspection predictions for selected modules at the Diablo Canyon ISFSI.

The COBRA-SFS code uses a finite-difference subchannel analysis approach for predicting flow and temperature distributions in spent fuel storage systems and fuel assemblies under forced and natural circulation flow conditions. It is applicable to both steady-state and transient conditions in single-phase gas-cooled spent fuel packages with radiation, convection, and conduction heat transfer. The code has been validated in blind pretest calculations using test data from spent fuel packages loaded with actual spent fuel assemblies as well as electrically heated single-assembly tests (Creer et al. 1987, Rector et al. 1986, Lombardo et al. 1986).

The data obtained in these on-site inspections provide an opportunity to develop structural and thermal models that can yield realistic predictions for actual storage systems, in contrast to conservative and bounding design-basis calculations. The analytical approach used in this study does not include many of the conservatisms and bounding assumptions normally used in design-basis and safety-basis calculations for spent fuel storage systems.

The primary storage modules used for this study consist of two selected modules in the Diablo Canyon Power Plant's ISFSI, designated as HI-STORM #318 and #516. Images of typical dry casks in place at the Diablo Canyon site can be viewed on the public internet site FLICKR, maintained and supported by Yahoo.com, at
http://www.flickr.com/photos/nrcgov/6871626011/in/photostream/

These images are from the U.S. Nuclear Regulatory Commission, a member of FLICKR since 2011, and are part of the NRCgov's photostream on this site, which currently runs to 1,393 images.

Figure 1-1 contains generic not-to-scale diagrams illustrating the major differences between the HI-STORM100 and HI-STORM100, Version B. A line drawing of a typical HI-STORM100 module is shown in Figure 1-2. The two modules selected for inspection are essentially identical, except for the multi-purpose canister (MPC) contents, which vary significantly in total decay heat load and loading pattern. Thermal models have been developed and evaluations performed for both modules, to have pre-inspection analyses for comparisons to data obtained from all the modules actually inspected.

The COBRA-SFS model geometry for the HI-STORM100S-218 Version B with MPC-32 canister is described in detail in Section 2. This section also presents the boundary conditions and modeling assumptions for the calculations to obtain predictions of long-term temperatures in the modules to be inspected at the Diablo Canyon ISFSI. Section 3 presents pre-inspection predictions of component temperatures and temperature distributions within the modules, based on the estimated decay heat loads in the fuel assemblies within the MPCs as of the planned inspection timeframe. A follow-on document will be issued post-inspection, which will include the pre-inspection results reported here as well as comparisons between pre-test predictions and inspection results, and further post-test calculations, if necessary, with appropriate discussion of results.

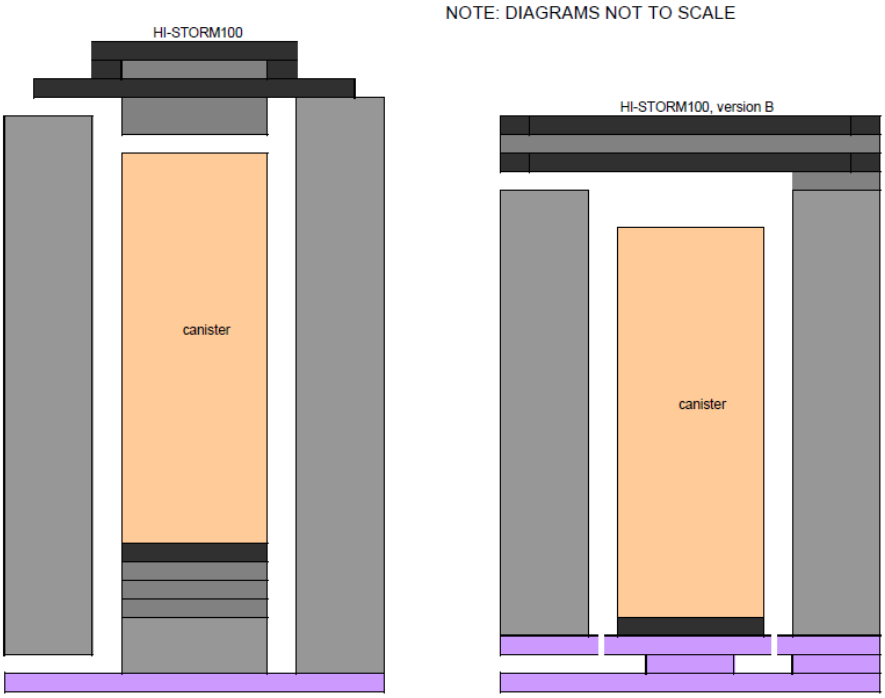

Figure 1-1. Generic Diagrams Illustrating Major Differences Between the HI-STORM100 and HI-STORM100 Version B Module Designs

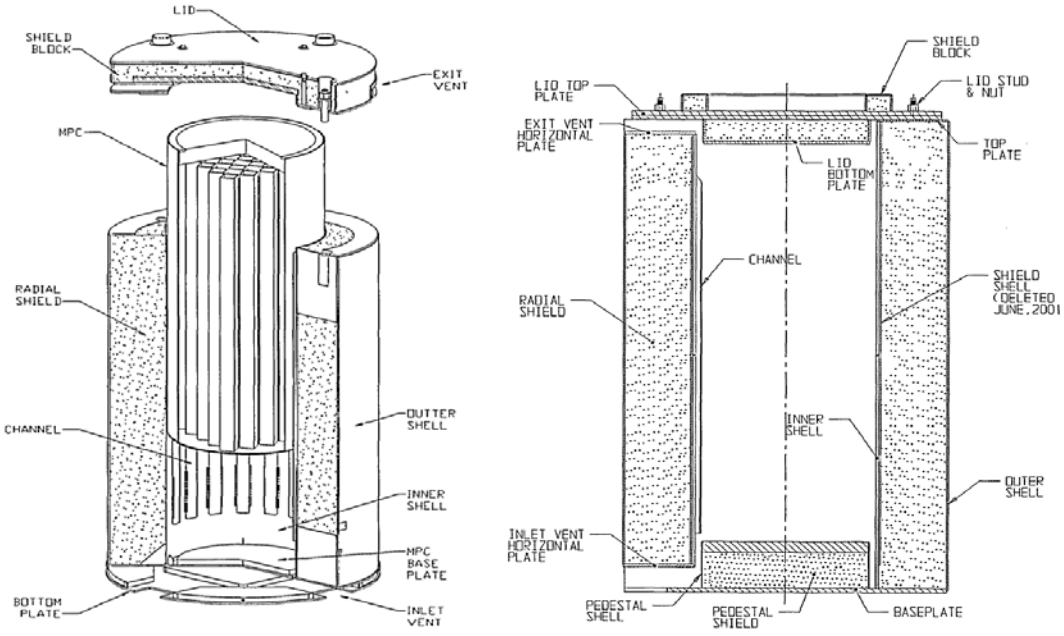

Figure 1-2. Typical HI-STORM 100S Vertical Storage Module (Image courtesy of Holtec International; reprinted with permission) NOTE: the 100-S-218 Version B design used at Hope Creek and the site-specific design at Diablo Canyon differ in some details from this image.

2.0 COBRA-SFS MODEL DESCRIPTION

The HI-STORM100 system is a vertical storage module design developed by Holtec International, and consists of an MPC inserted into a steel-lined concrete overpack (Holtec 2010). The general design of the overpack is similar for all configurations of the system, such that the main site-specific character of a particular installation is the design of the canister stored within the overpack. At the Diablo Canyon ISFSI, the canister design is the MPC-32, which is for pressurized water reactor (PWR) fuel, and stores up to 32 PWR fuel assemblies. The canisters in the storage modules to be inspected in the Diablo Canyon ISFSI are designated 02-02 and 03-05, in reference to loading of spent fuel into the canisters. The first number in the designation refers to the dry storage loading campaign number, and the second number identifies the cask in that campaign sequence. Casks in campaign 01 were loaded in June-August 2009; casks in campaign 02 were loaded in May-July 2010, and casks in campaign 03 were loaded in Jan-Feb 2012. The specific overpack modules these two canisters are loaded into are designated HI-STORM #318 (for 02-02) and HI-STORM #516 (for 03-05).

A COBRA-SFS model for a vertical storage system such as the HI-STORM 100 of whatever specific configuration consists of three major pieces; the canister, the air flow channel that allows external ambient air to circulate through the module, and the external overpack surrounding the canister. Information on the site-specific design of the modules at Diablo Canyon was not provided to PNNL before the actual inspection date, due to delays in implementing Non-Disclosure Agreements (NDAs) with the various parties involved. Therefore, for the pre-inspection thermal analysis of the selected modules at the Diablo Canyon ISFSI, the HI-STORM 100 overpack was modeled utilizing the COBRA-SFS model developed for the Hope Creek inspections (Cuta and Adkins, 2013). There are some significant differences between the 100S-218 Version B and the site-specific 100A configuration at Diablo Canyon. However, the general performance is similar for all of the various configurations of the HI-STORM100 overpack, since all modules are capable of accepting the full range of MPC designs developed by Holtec. Uncertainties in the pre-inspection thermal evaluation results, including uncertainties due to modeling assumptions, will be evaluated in the follow-on post-inpection report when analytical results are compared with the measured data obtained in the inspection.

The general structure of the model of the HI-STORM 100S-218 Version B storage system is illustrated in Figure 2-1. The detailed three-dimensional nodalization of the fuel assemblies, basket, canister, and overpack walls extends only over the axial length of the basket within the MPC. This highly detailed portion of the model represents the region of radial heat transfer from the fuel rods to the ambient environment. The axial length of this region is defined by the length of the basket, which in this case is assumed to be only 5.24 cm (2.06 inches) short of the total axial length of the canister internal cavity. Axial heat transfer out the top and bottom of the system is represented with a simpler, one-dimensional thermal resistance network, consisting of the upper and lower plenum regions.

Diagrams illustrating the model representation of the entire system are shown in Figures 2-2 and 2-3. For clarity, the canister and overpack portions of the model are shown separately. Figure 2-2 shows a cross-section diagram of the canister portion of the model, including the fuel rods, basket plates (with neutron poison plates), basket support structure, and canister shell. Different

colors are used for different components, for clarity in the complex mesh. This diagram is not to scale, since in a scaled diagram of the mesh, fine details such as the neutron poison plates are difficult to discern. In addition, the detailed rod-and-subchannel arrays within the basket cells are shown with the rod spacing greatly exaggerated, so that the subchannels are visible.

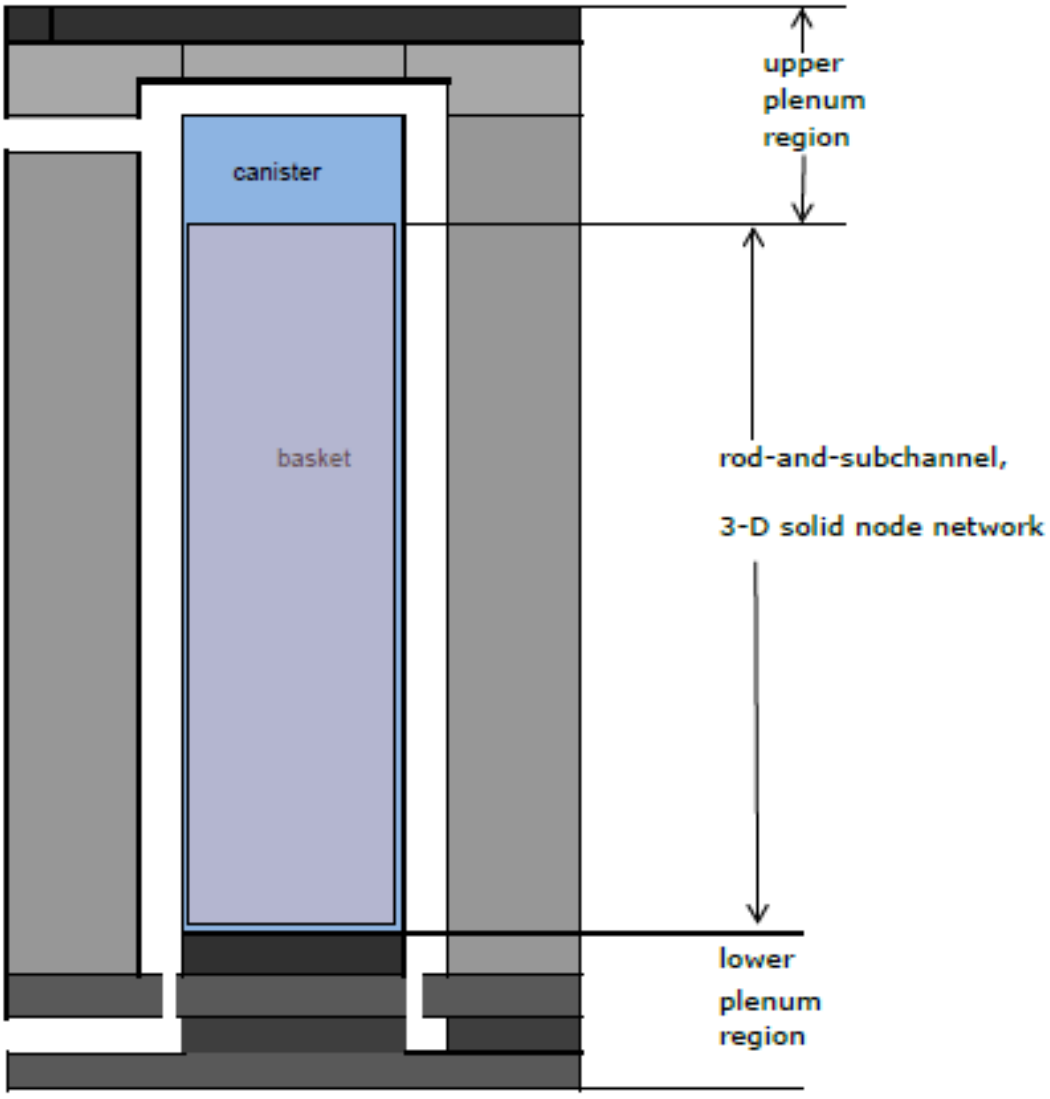

Figure 2-1. Diagram of Modeling Regions in COBRA-SFS Model of HI-STORM 100S-218 Version B Vertical Storage System (NOTE: diagram is not to scale)

Figure 2-3 shows a cross-section diagram of the portion of the model representing the overpack. The COBRA-SFS model includes channel shims on the inner wall of the overpack liner. Undocumented information on the Diablo Canyon ISFSI indicates that these shims are omitted in the modules at that site. However, the shims by design have minimal effect on the air flow in the annulus, as numerous licensing basis evaluations for systems of this design have shown. When full documentation is available for the site-specific design, this feature will be revised in the model developed for the post-inspection thermal analysis. It is not expected to have a large

effect on results. The geometry of both modules is essentially identical, and therefore the images in Figures 2-2 and 2-3 are applicable to the models for both modules to be inspected. The only significant difference in the models for the two modules is in the assembly loading pattern, which is unique for each module. The representation of the decay heat in the fuel assemblies in the COBRA-SFS model is discussed in detail in Section 2.1.

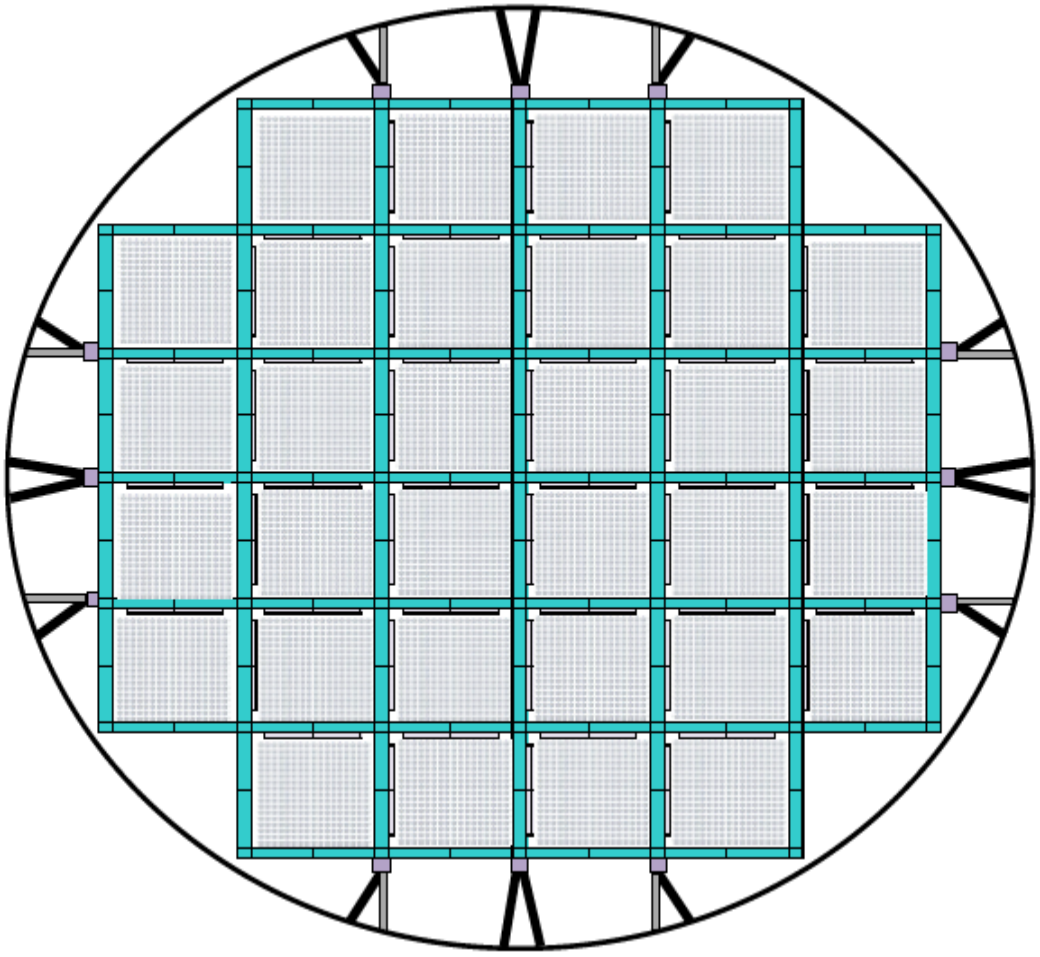

Figure 2-2. Diagram of 3-D COBRA-SFS Model of MPC-32 Canister in Thermal Model of Diablo Canyon Storage Module (NOTE: diagram not to scale; node thicknesses greatly exaggerated for clarity)

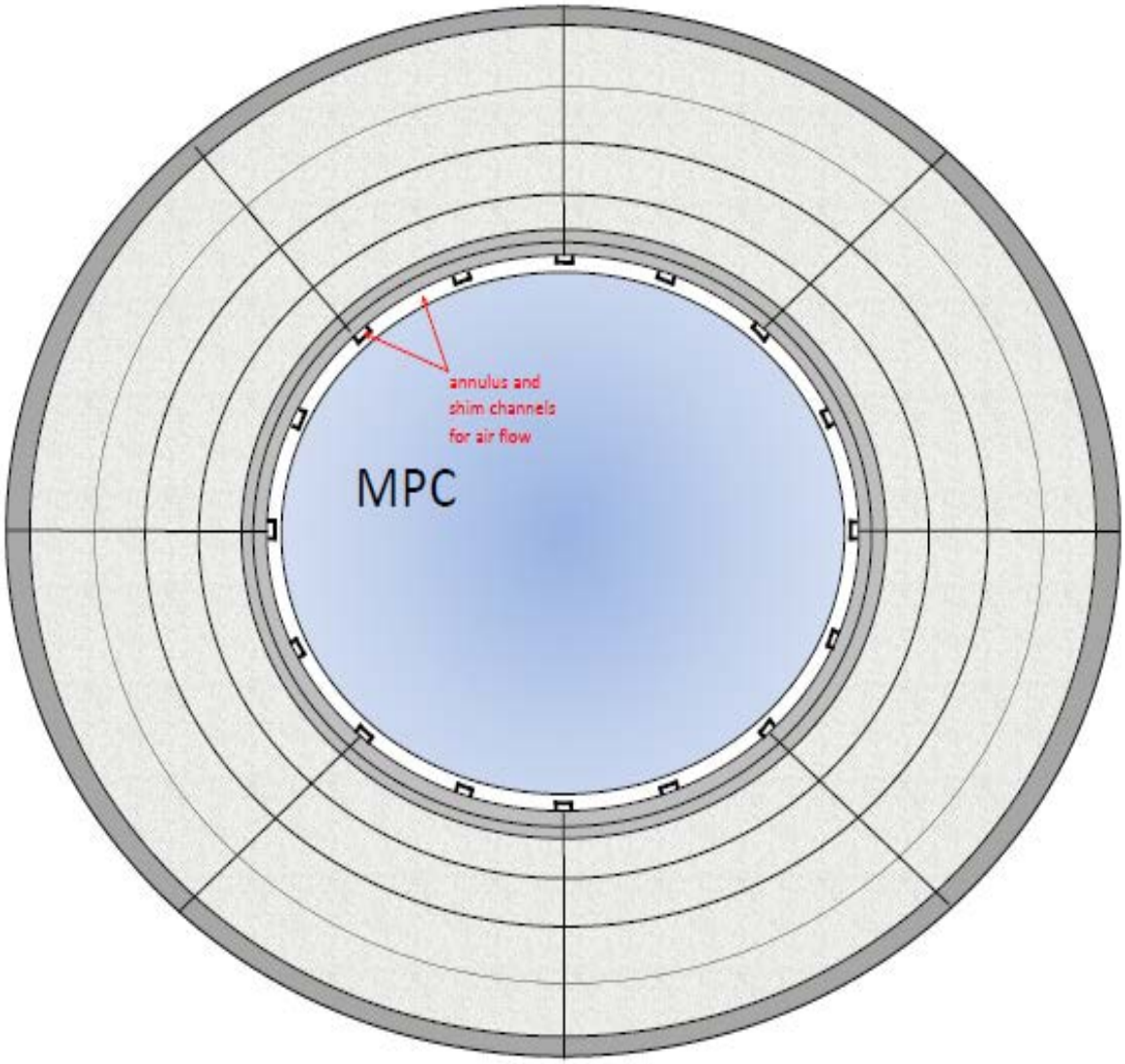

Figure 2-3. Cross-section of COBRA-SFS Model of Overpack for HI-STORM100S-218, Version B (diagram is not to scale. Air annulus width and steel thicknesses are greatly exaggerated for clarity.)

The detailed model of the canister and internals (including the fuel assemblies) shown in Figure 2-2 has the typical mesh resolution generally used for the basket structure in COBRA-SFS models of spent fuel storage systems. Finer mesh resolution can be specified, if needed, but comparison with temperature measurements from single assembly and multi-assembly experiments, including testing of storage systems with spent fuel loaded in the basket (Lombardo et al. 1986; Rector et al. 1986; Creer et al. 1987) has shown that this meshing is sufficient for resolution of temperature gradients typical of spent fuel storage systems. The mesh includes the basket plates, poison plates, and basket support structures, including the shims on these structures that are used to ensure firm contact between the basket frame and canister inner shell.

The thermal network approach used in COBRA-SFS allows direct representation of thin plates and the contact resistance due to small gaps between adjacent components. In typical models for CFD and finite element analysis (FEA) codes, structures consisting of adjacent thin plates (such as the basket plates, poison plates, and poison plate sheathing) are modeled as a single material with homogenized properties. The approach used in COBRA-SFS of modeling the individual thin plates and the appropriate contact resistances between them allows more detailed resolution of temperature distributions in such structures, using a comparatively smaller mesh.

As shown in Figure 2-2, the main feature of the COBRA-SFS model of the canister is the representation of the flow field within the fuel assemblies in the basket, and the flow paths external to the basket that allow recirculation due to natural convection within the canister. Within the individual basket cells, the fuel assembly and flow field is represented with a detailed subchannel model. This representation of the fuel assembly allows for much more accurate resolution of the local rod temperatures, compared to the typical approach used in CFD and FEA models, in which the fuel assembly region is represented as a homogeneous block with internal heat generation, or as a porous medium. The detailed rod and subchannel model allows the code to calculate individual fuel rod cladding temperatures, accounting for heat transfer by conduction, convection, and thermal radiation, and permits detailed modeling of material parameters, such as fuel cladding emissivity and surface conditions.

The detailed rod-and-subchannel array within a basket cell is illustrated in Figure 2-4 for a single WE 17x17 assembly. The fuel stored in the canisters of the Diablo Canyon ISFSI consist of two different configurations of WE 17x17 fuel; WE 17x17 Standard (STD) and WE 17x17 Vantage 5. These fuel designs have essentially the same physical geometry, but differ slightly in fuel rod diameter. The detailed COBRA-SFS model accounts for this geometry difference in the rod-and-subchannel model array in each of the basket cells of the canister. The two canisters evaluated each have a unique arrangement of the two different fuel types, as discussed in Section 2.1.

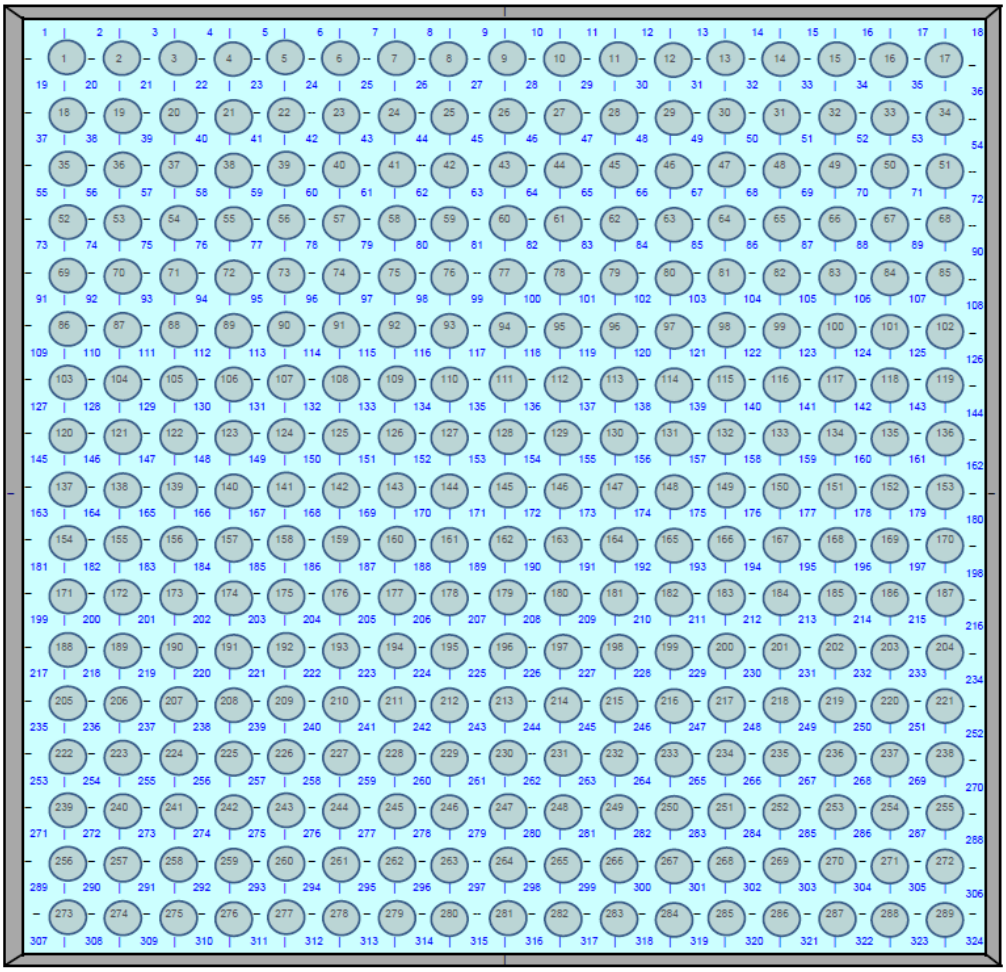

Figure 2-4. Rod-and-subchannel Array Diagram for COBRA-SFS Model of WE 17x17 Fuel Assembly within Basket Cell (Note: diagram is not to scale; rod spacing is greatly exaggerated for clarity.)

For convection heat transfer, the fluid channels within the canister are thermally connected to the fuel rods and to the surrounding solid conduction nodes representing the basket by means of a user-specified heat transfer correlation. Based on validation of the COBRA-SFS code with experimental data from vertical test systems and canisters loaded with actual spent fuel, convection heat transfer in the fuel rod array is represented with the venerable Dittus-Boelter heat transfer correlation for turbulent flow,

$$Nu = 0.023(Re^{0.8})(Pr^{0.4})$$

where Nu = Nusselt number
Re = Reynolds number, based on subchannel hydraulic diameter
Pr = Prandtl number for the backfill gas

For laminar flow conditions, a Nusselt number of 3.66 has been verified as applicable to spent fuel rod arrays. The local heat transfer coefficient is defined as the maximum of the values

calculated from the laminar and turbulent correlations specified by user input. Figure 2-5 illustrates the convenient mathematical behavior of these correlations as a function of Reynolds number.

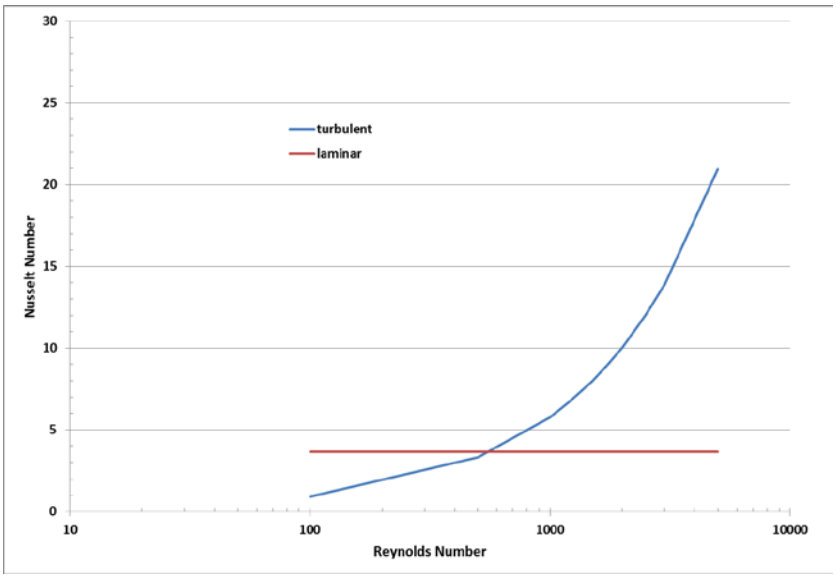

Figure 2-5. Laminar and Turbulent Formulations for Nusselt Number

In addition to convection heat transfer, the fluid energy equation includes conduction through the fluid (helium gas) in the subchannels, and the gas is assumed transparent to thermal radiation. Thermal radiation within the basket is calculated using 2-dimensional (planar cross-section) grey-body view factors for the rod array and surrounding solid conduction nodes of the basket wall. The view factors are calculated for the specific assembly and basket cell geometry using the auxiliary code RADGEN, which is part of the COBRA-SFS package. Thermal radiation across the geometrically simpler flow channels between the basket and the canister shell are determined in COBRA-SFS directly from user-input black body view factors, calculated using the Hottel crossed-string correlation methodology. Based on the specified surface emissivity of the nodes of the surfaces of a given flow region, the code calculates the grey-body view factors for thermal radiation exchange.

The annulus between the canister and the overpack is represented in the COBRA-SFS model with 20 flow channels to capture the circumferential variation in the annulus region cross-section due to the 16 shim channels spaced around the inner shell of the storage cavity (see Figure 2-3). As noted in Section 2.0 above, it has been reported informally that the modules at Diablo Canyon do not include these structures in the annulus. However, until the site-specific drawings for these modules are made available for model revisions (as anticipated for the post-inspection thermal evalutaions, when actual measured data is also made available), the shim channels have been retained in the COBRA-SFS module. These channels have a minimal impact on flow behavior in the annulus, and therefore their presence or absence is not expected to have any significant effect on predicted temperatures for the system.

The shim channels are open at top and bottom, and therefore constitute isolated flow paths for air circulation within the annulus. These flow paths are treated as separate parallel channels in the COBRA-SFS model. Air flow in the fluid channels representing the annulus is calculated using a pressure drop boundary condition based on the height of the system and the specified ambient air temperature. Momentum losses are determined using a friction factor correlation and form drag losses due to the orificing effects of the inlet and exit structures above and below the annulus.

Thermal connections between the annulus flow channels and the solid conduction nodes of the MPC shell, shim channel structures, and overpack inner shell are defined in the COBRA-SFS model for conduction and thermal radiation heat transfer. Convection heat transfer in the air annulus is treated as a forced convection flow, driven by the imbalance between the hydrostatic pressure drop within the annulus and that of the ambient air external to the overpack (Sparrow and Azevedo 1985). The Dittus-Boelter correlation has been shown to be an appropriate heat transfer model for prediction of heat transfer in a vertical storage module (Creer et al., 1987), but requires two minor modifications for application to the specific annulus geometry of the HI-STORM 100 system. The definition of the annulus hydraulic diameter used in the heat transfer correlation database is twice the radial width of the annulus (i.e., 2*W). The channel hydraulic diameter is defined in COBRA-SFS using the more general formula of four times the flow area divided by the wetted perimeter.

These two formulations are exactly equivalent for a simple circular annulus, but the base design of the HI-STORM 100 system contains 16 channel shims, to center the MPC within the overpack cavity (as illustrated in the diagram in Figure 2-3.) The presence of the shims effectively reduces the hydraulic diameter by approximately 50%, when calculated using the more general formula. However, evaluations by Holtec have validated appropriate agreement with heat transfer data in a vertical storage module (from Creer et al. 1987) using the Dittus-Boelter correlation for heat transfer in the annulus with the hydraulic diameter defined as 2*W and the Prandtl number coefficient[3] specified as 0.333. This is further confirmation that the presence or absence of the shim channels has minimal effect on hydrodynamics and heat transfer in the annulus, as long as the geometry is appropriately defined for the relevant correlations.

The equivalent formulation of this variation on the Dittus-Boelter correlation for COBRA-SFS is obtained by the simple expedient of doubling the leading coefficient of the correlation, and retaining the more appropriate general formulation of the Reynolds number based on actual hydraulic diameter of the flow channel. For the HI-STORM 100 annulus, the Nusselt number for turbulent flow heat transfer is specified as

$$Nu = 0.046\ Re^{0.8} Pr^{0.33}$$

where Re = Reynolds number, based on flow channel hydraulic diameter
Pr = Prandtl number for air

[3] The Dittus-Boelter correlation, which is derived with the general formulation $Nu = C\ Re^m Pr^n$, where C=0.023, m=0.8, and specifies n=0.4 for heating and n=0.3 for cooling. The original database did not investigate the effects of heating on one wall and cooling on the other, as is the situation in the HI-STORM 100 annulus.

The air flow in the annulus is expected to be turbulent for normal conditions of storage, but the COBRA-SFS input also includes a lower bound of Nu = 7.44 (derived[4] from Sparrow et al., 1961), which represents laminar flow conditions in a vertical stack. As illustrated in Figure 2-5, the code uses the mathematical behavior of the correlations to automatically select the appropriate flow regime by taking the maximum of the values obtained with the laminar and turbulent formulations for the local flow conditions.

2.1 Fuel Assembly Decay Heat Modeling

The spent fuel stored at the Diablo Canyon ISFSI consists of WE 17x17 assemblies in two slightly different configurations, designated STD and Vantage 5, as noted above in the discussion of fuel assembly geometry modeling with COBRA-SFS. The significant difference between the two designs is the diameter of the active fuel rods, which is slightly smaller in the Vantage 5 fuel. Both configurations have nominally 289 pin positions within the array, with 264 active fuel rods. Information provided by PGE[5] included the individual assembly decay heat loads at the time of loading into an MPC, cooling time as of time-of-loading, initial enrichment, assembly burnup, and assembly load maps for the canisters in dry storage at the ISFSI, including all modules being considered for inspection.

The methodology used by PGE to determine the individual assembly decay heat values at loading is not specifically referenced, but has been informally identified as a conservative evaluation based on ORIGEN calculations. The decay heat values at the time of the planned inspections were estimated from the 'at loading' decay heat values by performing calculations with the Used Nuclear Fuel Storage, Transportation, Disposal Analysis Resources and Data system (UNF-ST&DARDS) (Peterson et al., 2013). These calculations obtained decay heat values in these fuel assemblies as of December 2013, the originally scheduled timeframe of the inspections at the Diablo Canyon ISFSI.

The total canister decay heat loadings for the two modules inspected are summarized in Table 2-1. The decay heat values calculated for all assemblies within the individual canisters are listed in Table 2-2. (The basket location of an assembly is identified by row number and column letter, using the convention illustrated in the diagram in Figure 2-6.) These tables include the values reported for the time of loading and values calculated for the time of the inspection, originally scheduled for December 2013. The time of actual inspection, in January 2014, is close enough to December 2013 for the change in decay heat over that one-month time interval to be well within the uncertainty of the modeling.

Table 2-1. Total Decay Heat Loading per Module

	ORIGEN	
	decay heat (kW)	
Module	**at loading (date)**	**at inspection (estimated as 12/2013)**
#318 (02-02)	20.10 (5/17/2010)	17.05
# 516 (30-05)	15.39 (2/13/2012)	13.87

[4] The mean value in the reference is Nu=7.86. The value of 7.44 represents the lower bound on the ±5% uncertainty in the data.

[5] Provided in spreadsheet 'Info on Assemblies In ISFSI.xls', sheet 'All Campaigns – reviewed', transmitted as an attachment to e-mail from Keith Waldrop of EPRI (sent Thursday 4/25/2013 12:05pm PDT).

Table 2-2. Assembly Decay Heat Loadings for Modules Inspected at Diablo Canyon ISFSI

Basket cell location	Assembly decay heat (W)			
	at time of loading		December 2013 (inspection timeframe)	
	Module #318 (02-02)	Module # 516 (30-05)	Module #318 (02-02)	Module # 516 (30-05)
B-1	520.4	407.41	467.0	372.07
C-1	529.6	380.34	451.7	349.80
D-1	544.9	378.31	481.7	347.51
E-1	553.9	379.2	491.8	345.48
A-2	566.1	302.61	501.9	275.87
B-2	567.1	410.42	503.8	374.82
C-2	580.3	618.6	513.7	552.54
D-2	777.6	620.62	602.9	554.10
E-2	568.1	416.48	502.6	381.50
F-2	520.6	361.13	457.1	331.61
A-3	550.9	409.42	488.8	375.16
B-3	834.2	614.56	641.7	549.27
C-3	855.8	663.16	659.5	560.65
D-3	801.3	679.86	621.5	604.70
E-3	752.5	620.64	649.1	552.91
F-3	535.2	362.14	452.9	333.27
A-4	540.8	374.27	479.6	344.24
B-4	773.2	617.61	618.3	551.57
C-4	808.4	654.81	626.4	553.64
D-4	633.5	680.86	544.2	608.18
E-4	778.5	626.71	649.8	559.98
F-4	547.9	378.32	485.7	348.15
A-5	524.6	401.36	463.8	367.68
B-5	578.2	410.43	513.4	374.98
C-5	795.1	616.61	617.1	550.60
D-5	756.6	635.77	652.6	567.78
E-5	572.2	434.28	508.1	404.24
F-5	558	356.09	495.2	328.89
B-6	563	380.21	499.1	350.87
C-6	548.9	379.21	486.6	348.69
D-6	538.8	407.41	476.0	375.67
E-6	524.5	406.39	447.7	372.59

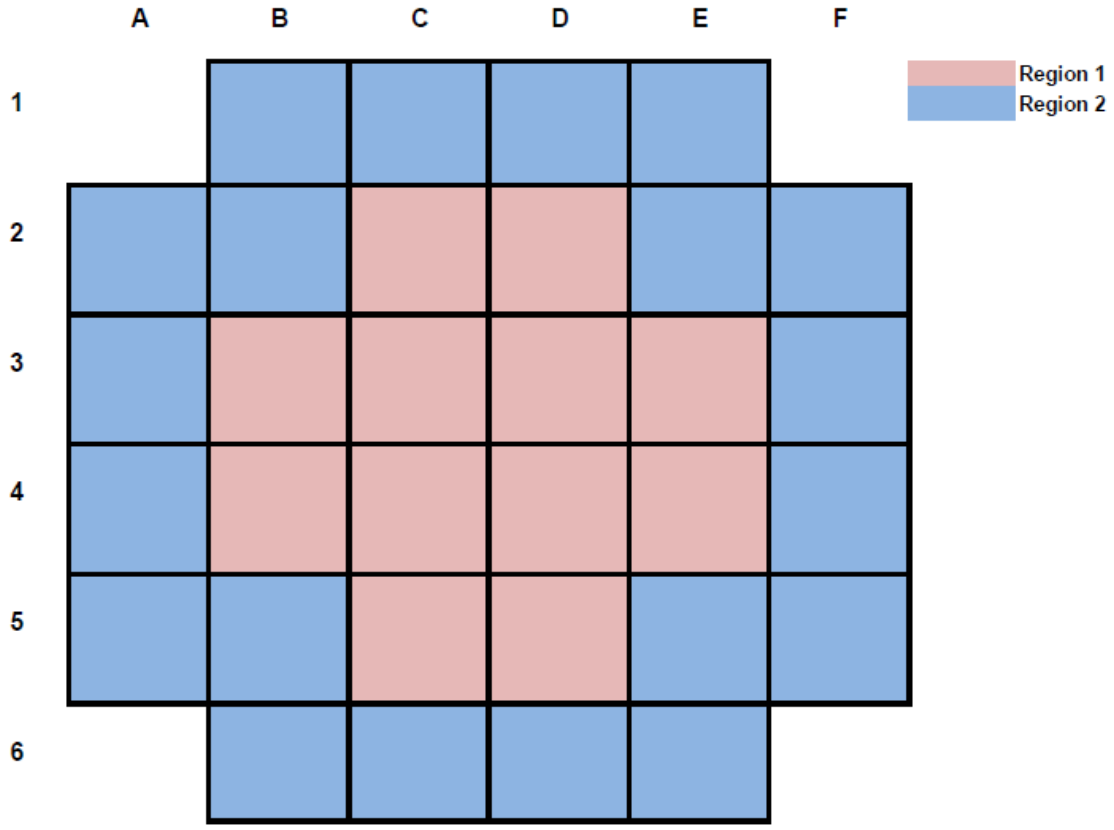

Figure 2-6. Diagram Illustrating Basket Cell Location Convention

The axial decay heat distribution for the WE 17x17 fuel within the canisters was modeled with a generic profile for PWR fuel, since axial burnup distributions for the fuel were not included in the fuel data package. This profile, shown in Figure 2-7, is a bounding profile determined for low burnup PWR spent fuel (DOE 1998). More accurate information on the axial decay heat profile would result in more accurate predictions of peak component temperatures within the canister. Because the profile for spent fuel is relatively flat, the uncertainty in peak temperature predictions due to this approximation is probably rather small. Near the ends of the fuel region, however, the profile is expected to drop to near zero over a relatively short distance. This gradient strongly influences the temperature profile near the ends of the canister. The generic profile, rather than profiles representative of the fuel stored in these modules, is a potential source of uncertainty in the predictions of axial temperature distribution in the thermal modeling.

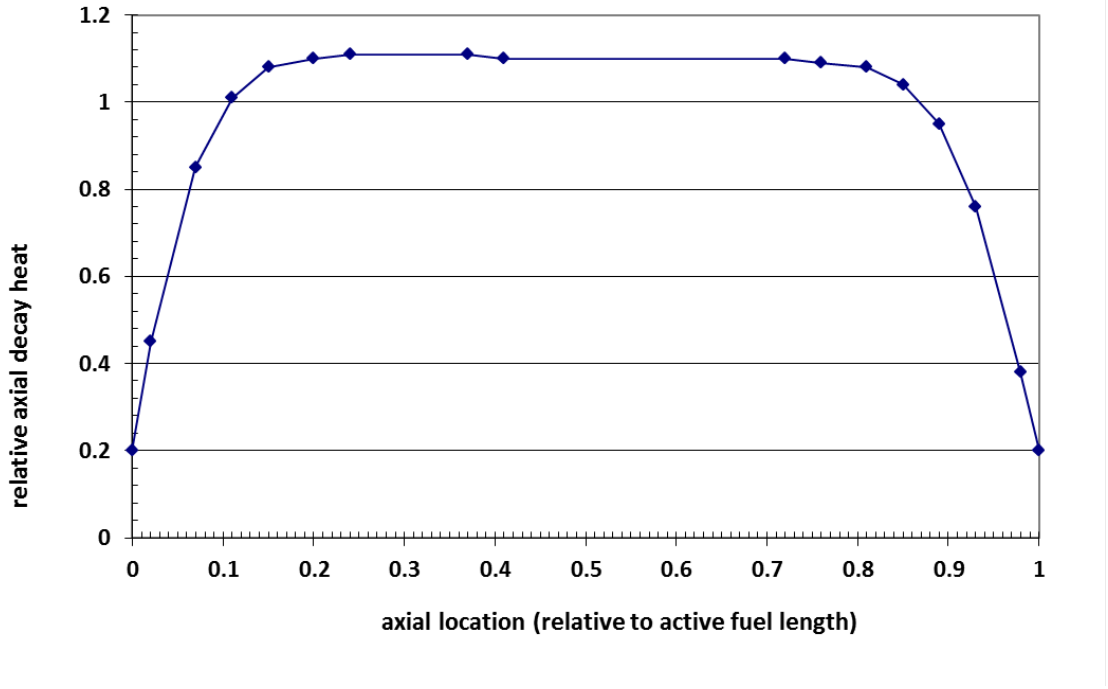

Figure 2-7. Bounding Axial Decay Heat Profile for low burnup PWR Spent Fuel (DOE 1998)

2.2 Ambient Conditions

Ambient conditions at the ISFSI, including air temperature and local surface winds, at the time of the inspection are expected to have a significant effect on the temperatures that will be measured in the storage module. The inspection plans include inserting a specially designed thermal probe through an exit vent and down into the annulus, and obtaining outer shell surface temperature measurements along the axial length of the canister. Because the primary mode of heat removal from the canister at the outer shell is convection to the air flowing up the annulus, the shell surface temperature is directly dependent on the inlet air temperature.

For the pre-inspection evaluations, since it is not known what the air temperature will be at the time of the inspection, an average ambient temperature of 50°F (10°C) was assumed in these calculations. For comparison, calculations were also performed at 80°F (27°C), which is the design basis ambient air temperature for the HI-STORM 100 systems. Additional calculations were performed assuming ambient temperatures of 70°F (21°C), 60°F (16°C) and 40°F (4°C). Based on data[6] obtained from the National Oceanic and Atmospheric Administration (NOAA 2013), this range is typical for winter temperatures in the mild climate of southern California. This is illustrated by the plot in Figure 2-8, showing daily maximum, minimum, and average temperatures for December 2012 recorded by the National Weather Service Forecast Office at the Los Angeles/Oxnard office. Historical maximum temperatures for the region have reached as high as 85°F (29°C), and record lows have dropped as low as 20°F (-7°C), but generally do

[6] This data will be archived after final quality control review (after the end of 2013), by the National Climatic Data Center (NCDC), and will be publicly available at http://www.ncdc.noaa.gov.

not fall below 30°F (-1°C) for December. This suggests that the selected temperature range for these evaluations is likely to span the actual conditions at the site during the inspections.

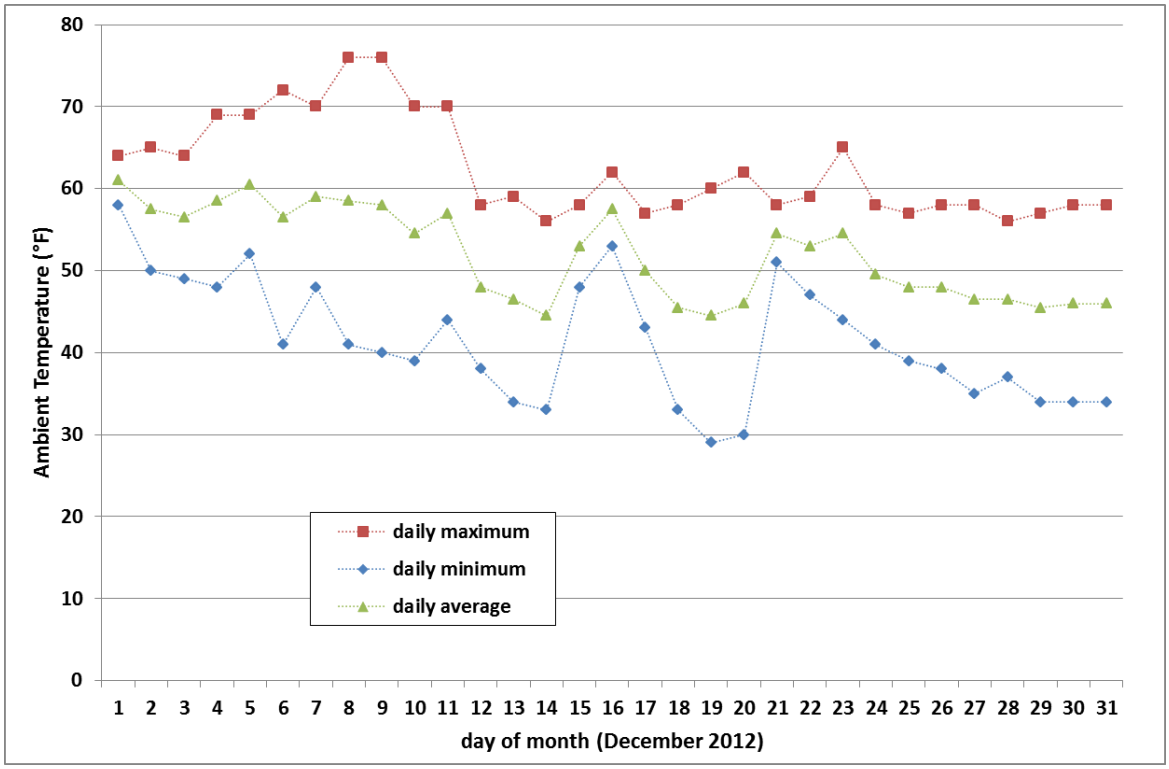

Figure 2-8. Daily Maximum, Minimum, and Average Temperatures Reported for San Luis Obispo, CA in December 2012 (NOAA 2013)

The temperature data shown in Figure 2-8 is archived data from a National Weather Service reporting station in San Luis Obispo, approximately 8 miles northeast of the Diablo Canyon site. Ambient temperature data from a monitoring station located at the ISFSI would yield a more accurate estimate of local ambient conditions, but such data is not available for pre-inspection evaluations.

In all cases, these ambient conditions assume still air. Consideration of wind effects in the current modeling effort would require detailed information on wind speed, direction, and variation over time at the ISFSI location, to estimate the effect on flow velocities at the inlet vents of the specific modules to be inspected. By definition, this information is not available for pre-inspection calculations. The study of wind effects on storage system performance is a topic of some interest in general for a number of reasons, but it is beyond the scope of the current work.

The external solar heat load on the modules assumed for these calculations is based on the solar radiation assumptions specified in 10 CFR 71.71 (10 CFR 71). This regulation is specifically for transport conditions, but the specified values are generally used for stationary storage systems, as well. Solar radiation over a 12-hour period is defined in 10 CFR 71.71 as

- 800 cal/cm^2 (2950 Btu/ft^2) for horizontal surfaces
- 400 cal/cm^2 (1475 Btu/ft^2) for curved surfaces.

Adjusting for the surface emissivity, which in these evaluations is assumed to be 0.9 for the painted exterior surfaces of the overpack, the above specified values are averaged over a 24-hour period, to obtain the following solar heat flux values for this system:

- 349 W/m^2 (110.6 Btu/hr-ft^2) on the overpack lid
- 175 W/m^2 (55.3 Btu/hr-ft^2) on the outer shell.

These values may be conservative for the solar heat load on the modules at the time of the actual inspection, but in the absence of site-specific information, they will have to do.

3.0 PRE-INSPECTION PREDICTIONS OF COMPONENT TEMPERATURES

The COBRA-SFS model described in Section 2 was used to obtain predictions of component temperatures within the two modules to be inspected at the Diablo Canyon ISFSI. These calculations assume an average ambient temperature of 50°F (10°C), in still air, with external solar heat load as specified in 10 CFR 71. Table 3-1 summarizes peak temperatures predicted for components of the canister for each case. Table 3-2 summarizes peak temperatures predicted for components of the overpack.

Table 3-1. Peak Component Temperatures, °F (°C), in MPCs (ambient 50°F (10°C))

Module	Fuel cladding	Neutron Poison Plate	Basket plate	Basket periphery	Basket support	Canister inner surface	Canister outer surface
#318 (02-02)	357.2 (180.7)	352 (177.6)	352 (177.6)	297 (147.4)	284 (140.0)	237 (113.6)	235 (113.0)
#516 (03-05)	312.6 (155.9)	307 (152.7)	307 (152.7)	259 (126.3)	248 (120.1)	208 (97.8)	207 (97.3)

Table 3-2. Peak Component Temperatures, °F (°C), in Overpack (ambient 50°F (10°C))

Module	Overpack inner shell	Overpack concrete	Overpack outer shell	Overpack lid inner surface	Overpack lid outer surface
#318 (02-02)	110 (43.2)	107 (41.7)	61 (15.8)	65 (18.1)	64 (17.6)
#516 (03-05)	100 (37.6)	98 (36.4)	60 (15.6)	64 (18.0)	64 (17.6)

Axial temperature distributions on the canister shell are presented in Figures 3-1 through 3-2 for the two modules. (Tabular values for all plotted axial profiles are provided in Appendix A.) These plots show temperatures at two different radial locations, to illustrate the non-uniform circumferential temperature variation on the canister shell, due to the basket configuration within the MPC-32. The “square peg in a round hole” geometry of the rectilinear basket within the cylindrical canister results in relatively large open gaps between the basket corners and the canister shell, as illustrated in Figure 2-2, which shows the noding diagram for the COBRA-SFS model of the basket region. The flat ‘faces’ of the basket are physically closer to the wall, and also have direct conduction heat transfer paths to the outer shell through the metal of the basket support structures. The modules at Hope Creek , in contrast, showed very little variation in circumferential variation in predicted canister shell temperatures (Cuta and Adkins, 2013), mainly because the MPC-68 basket more completely fills the circular cross-section of the canister, resulting in a more uniform circumferential heat flux distribution on the canister shell. The MPC-68 basket has twice as many support structures (24, compared to only 12 in the MPC-32), which provide direct contact points for conduction heat transfer between the basket plates and the canister shell. The effect of the smaller MPC-32 basket on the circumferential temperature distribution at the canister surface is illustrated more clearly by the plots shown in Figures 3-3 and 3-4 for the two Diablo Canyon modules.

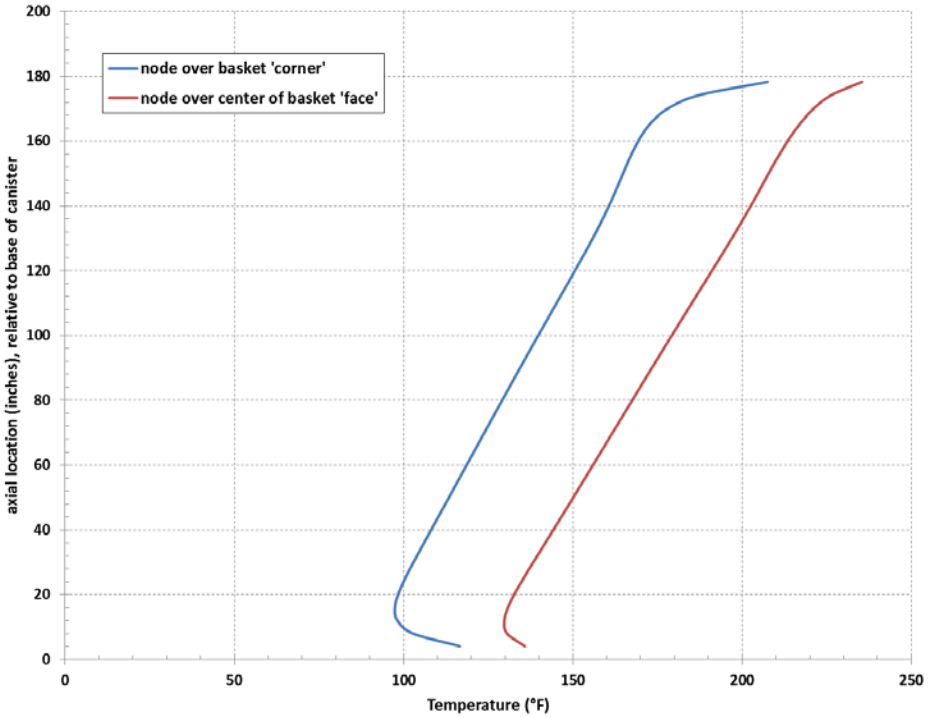

Figure 3-1. Axial Temperature Profiles on MPC Outer Shell: Module #318 (02-02), 50°F (10°C) ambient

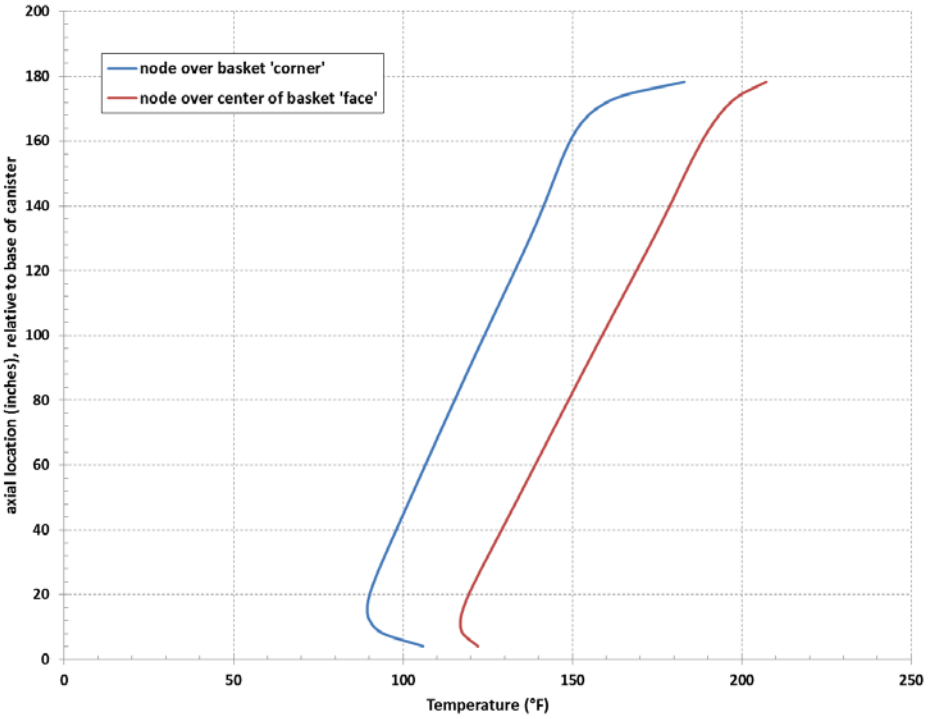

Figure 3-2. Axial Temperature Profiles on MPC Outer Shell: Module #516 (03-05) (50°F (1°C) ambient

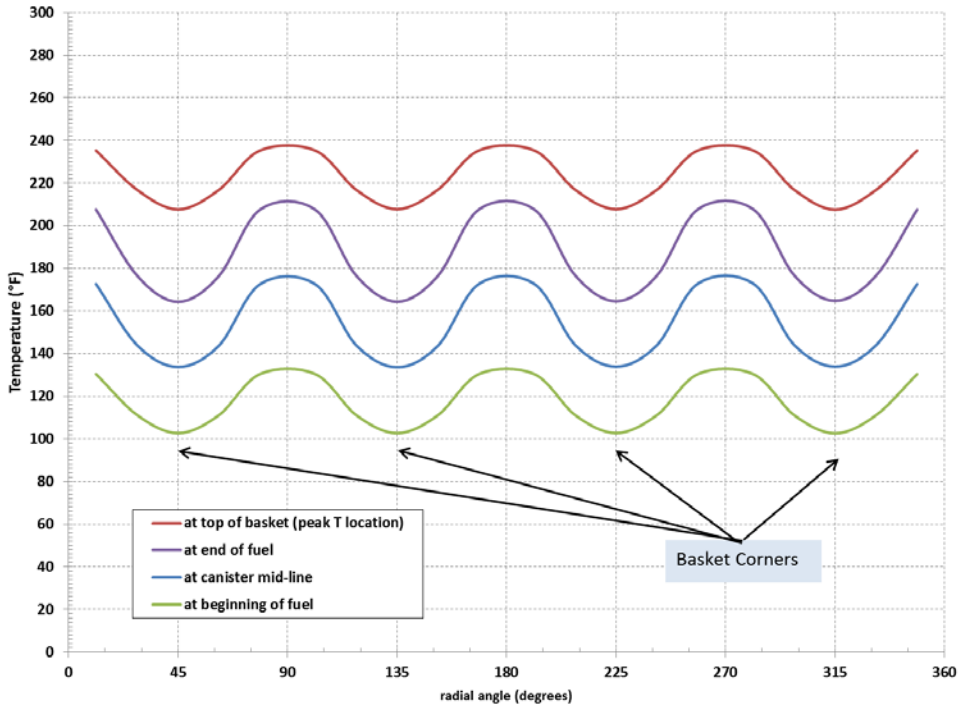

Figure 3-3. Circumferential Temperature Distributions on MPC Outer Shell: Module #318 (02-02), 50°F (10°C) ambient

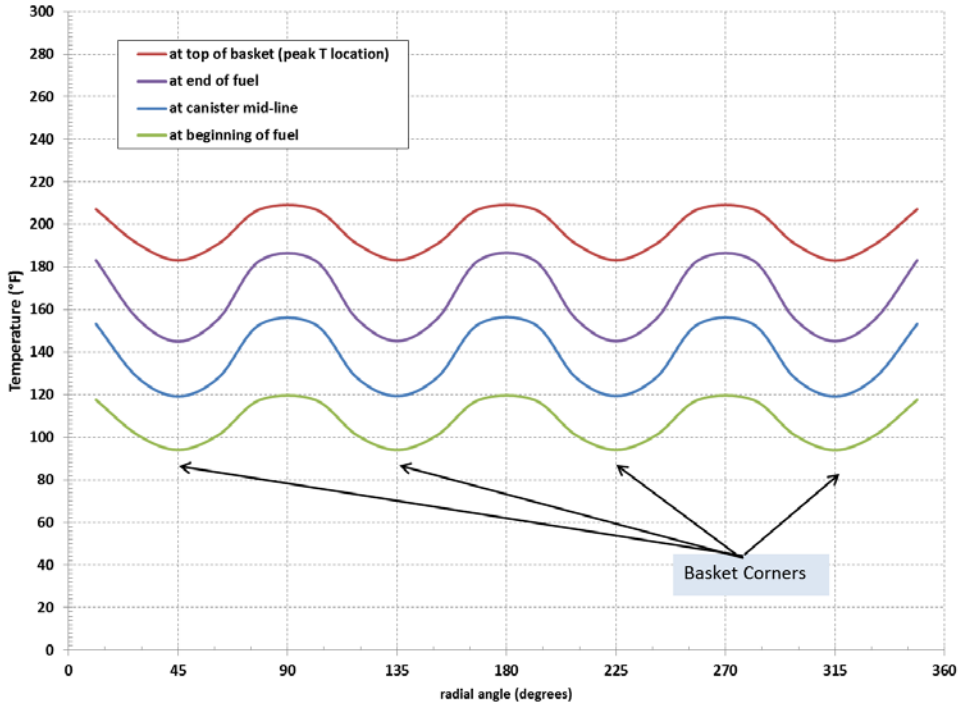

Figure 3-4. Circumferential Temperature Distributions on MPC Outer Shell: Module #516 (03-05) (50°F (10°C) ambient

An additional factor influencing the circumferential variation in predicted temperatures is the fuel loading pattern within the canister basket. The distribution of the decay heat load in the 02-02 and 03-05 canister baskets places 'colder' fuel assemblies in the basket corners, for radiation self-shielding. This is illustrated in Figures 3-5 through 3-8, with plots of the decay heat values (from ORIGEN calculations for December 2013) for the assemblies within the basket. (Refer to Figure 2-6 for basket row/column cell numbering convention.)

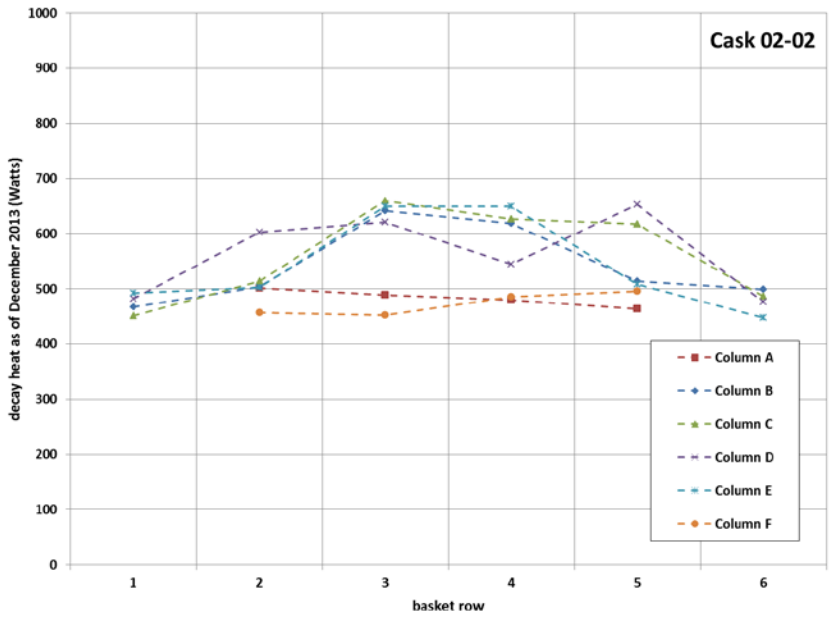

Figure 3-5. Assembly Decay Heat Distribution in Basket of Canister 02-02

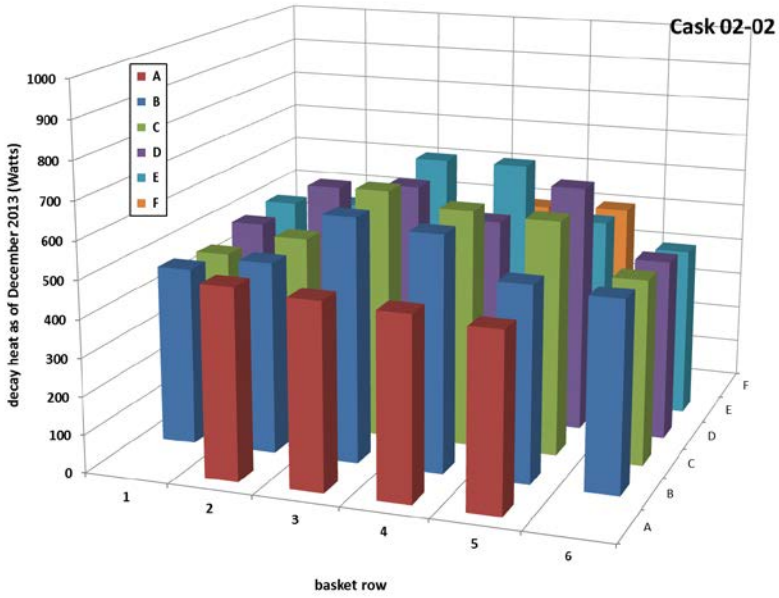

Figure 3-6. 3-D Illustration of Assembly Decay Heat Distribution in Basket of Canister 02-02

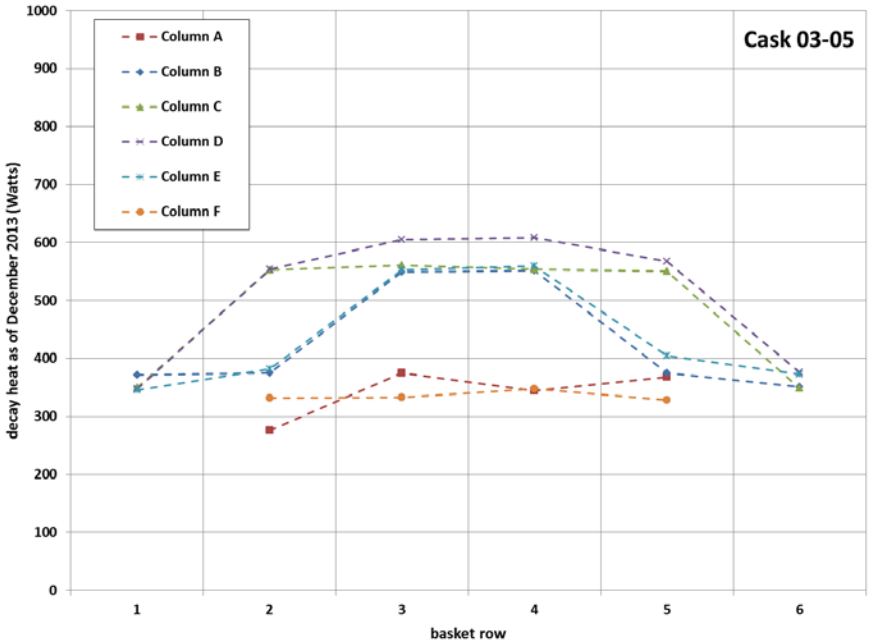

Figure 3-7. Assembly Decay Heat Distribution in Basket of Canister 03-05

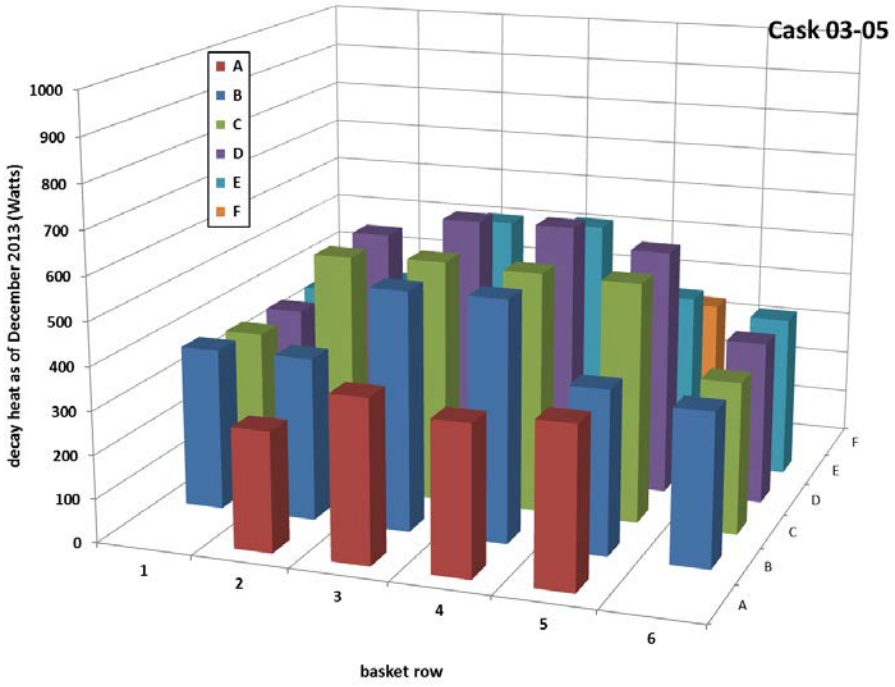

Figure 3-8. 3-D Illustration of Assembly Decay Heat Distribution in Basket of Canister 03-05

The line graphs in Figures 3-5 and 3-7 show the numerical values summarized in Table 2-2 for the two canisters. The column charts provide a more visual illustration of the non-uniform distribution of assembly decay heat values, showing the reduced heat load in the basket 'corners'. Table 3-3 summarizes the maximum, minimum, and average assembly decay heat values for the assemblies in these two canisters. (Refer to Figure 2-6 for location convention.)

Table 3-3. Summary of Decay Heat Variation from Basket Center to Periphery (from December 2013 Calculated Assembly Decay Heat Values)

Module	peak assembly		coldest assembly		Region 1 average assembly decay heat (Watts)	Region 2 average assembly decay heat (Watts)
	(Watts)	location	(Watts)	location		
#318 (02-02)	660	C-3 (Region 1)	448	B-1 (Region 2)	616	483
#516 (03-05)	608	D-4 (Region 1)	276	A-2 (Region 2)	564	355

The predicted temperatures for the storage modules are sensitive to the ambient temperature, and there is some uncertainty in the possible range of the ambient temperature at the time of inspection. Therefore, an additional set of cases were run to provide temperature predictions for assumed daytime ambient temperatures of 80°F (26.7°C), 70°F (21.1°C) , 60°F (15.6°C), and 40°F (4.4°C). Tables 3-4 and 3-5 show the effect of the variation in this boundary condition on the peak temperatures predicted for the two modules. Figure 3-9 shows the effect on the canister shell temperature profiles for Module #318 (02-02). Figure 3-10 shows the effect for Module #516 (03-05). (Tabular values for all plotted axial profiles are provided in Appendix A.)

Table 3-4. Effect of Ambient Temperature on MPC Peak Component Temperatures, °F (°C)

ambient temperature	fuel cladding	Fuel channel	basket plate	basket periphery	basket support	canister inner surface	canister outer surface
Module #318 (02-02)							
40°F (4°C)	345.8 (174.3)	340 (171.2)	340 (171.2)	288 (142.1)	274 (134.2)	226 (107.5)	224 (106.9)
50°F (10°C)	357.2 (180.7)	352 (177.6)	352 (177.6)	297 (147.4)	284 (140.0)	237 (113.6)	235 (113.0)
60°F (16°C)	369 (187.2)	363 (184.1)	363 (184.1)	307 (152.9)	295 (146.0)	248 (119.9)	247 (119.3)
70°F (21°C)	380.5 (193.6)	375 (190.5)	375 (190.5)	317 (158.4)	305 (151.8)	259 (125.9)	258 (125.4)
80°F (27°C)	392 (200.0)	386 (196.8)	386 (196.8)	327 (164.1)	316 (157.6)	270 (132.0)	269 (131.4)
Module #516 (03-05)							
40°F (4°C)	301.2 (149.6)	296 (146.4)	296 (146.4)	250 (120.8)	238 (114.3)	197 (91.8)	196 (91.3)

50°F (10°C)	312.6 (155.9)	307 (152.7)	307 (152.7)	259 (126.3)	248 (120.1)	208 (97.8)	207 (97.3)
60°F (16°C)	324.2 (162.3)	319 (159.2)	319 (159.2)	269 (131.9)	259 (126.1)	219 (104.0)	218 (103.5)
70°F (21°C)	335.6 (168.7)	330 (165.5)	330 (165.5)	280 (137.6)	269 (131.9)	230 (110.1)	229 (109.6)
80°F (27°C)	347 (175.0)	341 (171.9)	341 (171.9)	290 (143.2)	280 (137.7)	241 (116.1)	240 (115.6)

It is important to note that the temperatures reported here are based on steady-state calculations in still air. This analysis does not capture the effect of diurnal temperature variation throughout the system, or variation in wind conditions and solar heat load. Thermal inertia will tend to slow the rate of change of temperatures on canister internal components in response to ambient conditions (specifically, the peak fuel cladding temperature, peak fuel channel temperature, and hottest basket plate). However, the canister shell temperature, which is directly cooled by ambient air flowing in the annulus, is expected to track local ambient fairly closely, and therefore the ambient temperature and wind conditions will have an effect on the measured temperatures at the time of the inspection.

Table 3-5. Effect of Ambient Temperature on Overpack Peak Component Temperatures, °F (°C)

ambient temperature	**overpack inner shell**	**overpack concrete**	**overpack outer shell**	**overpack lid inner surface**	**overpack lid outer surface**
Module #318 (02-02)					
40°F (4°C)	98(36.9)	96 (35.5)	51 (10.3)	55 (12.6)	54 (12.1)
50°F (10°C)	110 (43.2)	107 (41.7)	61 (15.8)	65 (18.1)	64 (17.6)
60°F (16°C)	121 (49.6)	119 (48.1)	71 (21.4)	75 (23.7)	74 (23.1)
70°F (21°C)	133 (55.9)	130 (54.4)	80 (26.9)	85 (29.2)	84 (28.7)
80°F (27°C)	144 (62.3)	141 (60.8)	90 (32.5)	94 (34.7)	94 (34.2)
Module #516 (03-05)					
40°F (4°C)	89 (31.4)	86 (30.3)	50 (10.1)	55 (12.5)	54 (12.1)
50°F (10°C)	100 (37.6)	98 (36.4)	60 (15.6)	64 (18.0)	64 (17.6)
60°F (16°C)	111 (43.8)	109 (42.6)	70 (21.2)	74 (23.6)	74 (23.1)
70°F (21°C)	122 (50.1)	120 (48.8)	80 (26.7)	84 (29.1)	84 (28.7)
80°F (27°C)	133 (56.3)	131 (55.0)	90 (32.3)	94 (34.6)	94 (34.2)

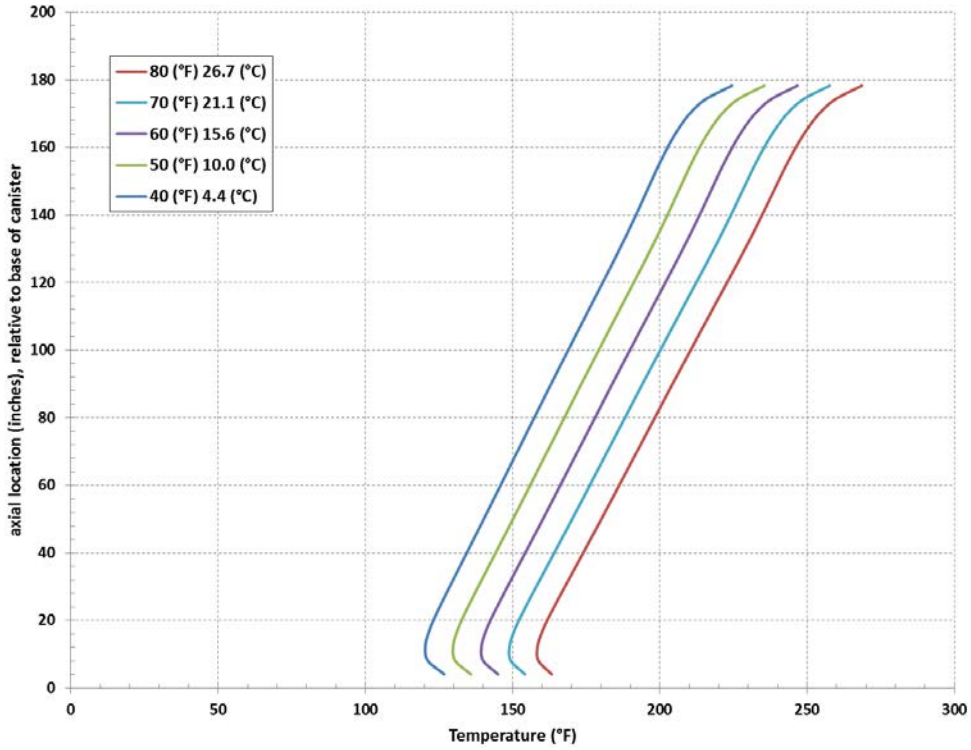

(a) basket 'face' profiles

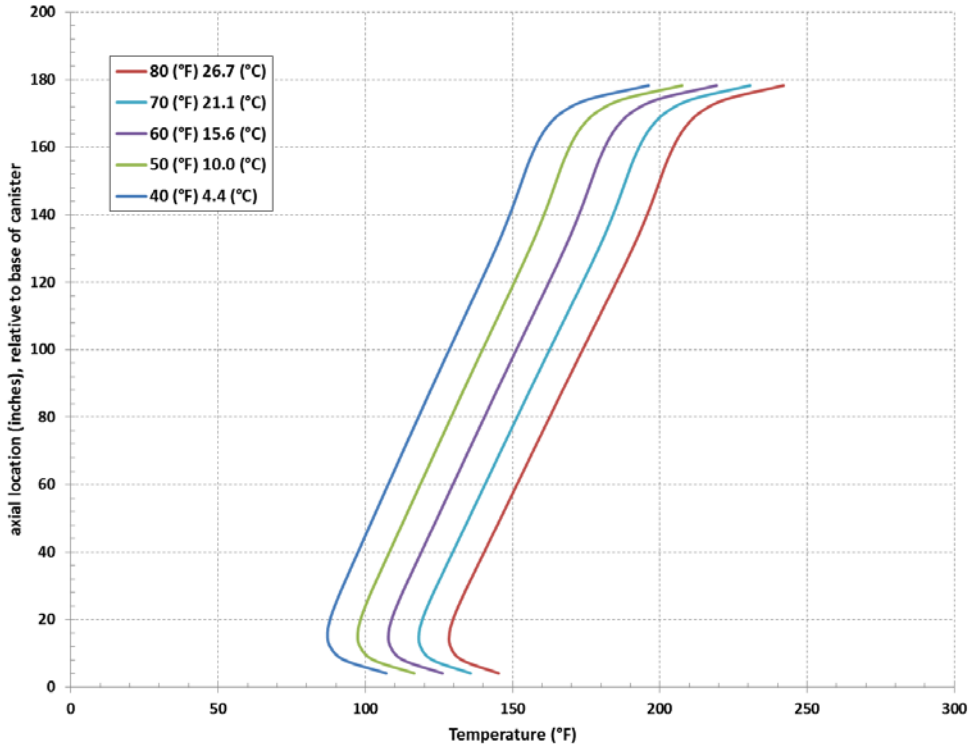

(b) basket corner profiles

Figure 3-9. Axial Temperature Profiles on MPC Outer Shell for Module #318 (02-02) for Range of Ambient Temperatures (a) at basket 'face', and (b) at basket corner

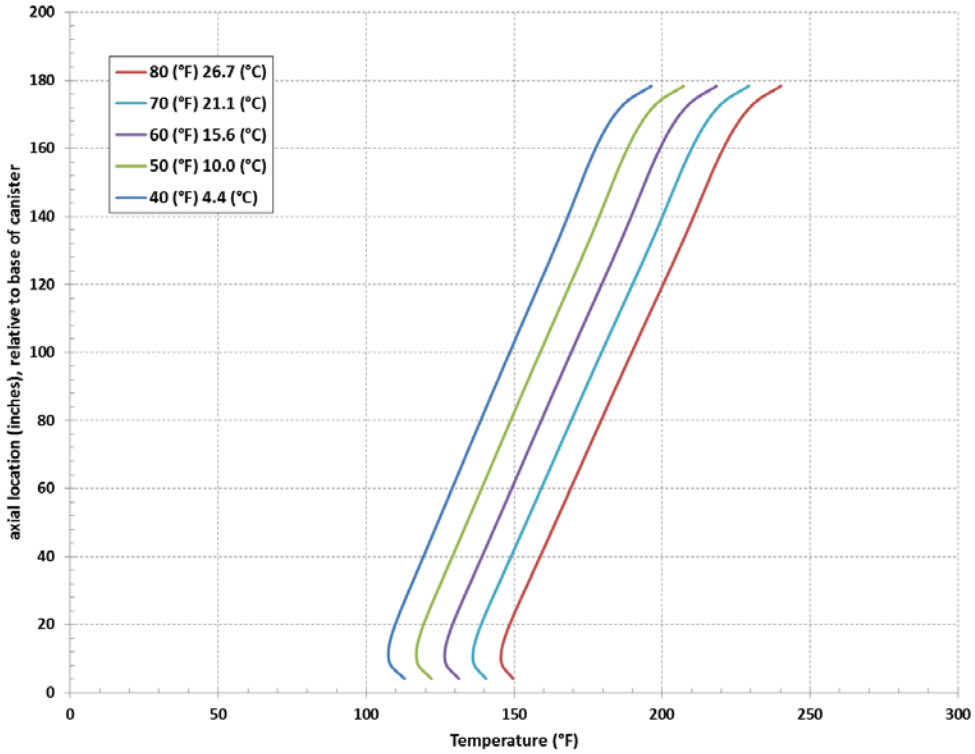

(a) basket 'face' profiles

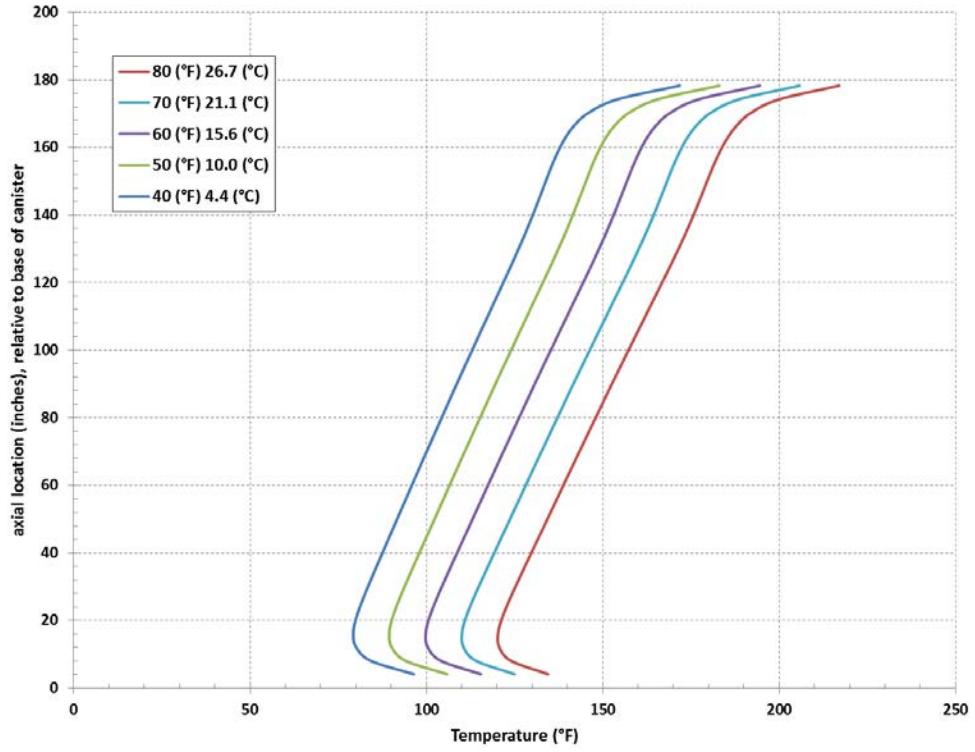

(b) basket corner profiles

Figure 3-10. Axial Temperature Profiles on MPC Outer Shell for Module #516 (03-05) for Range of Ambient Temperatures (a) at basket 'face', and (b) at basket corner

4.0 CONCLUSIONS

Conclusions relevant to this work will depend on the results of the inspections, and post-inspection evaluations of temperature measurements obtained in the specific modules. These will be documented in a separate follow-on report, to be issued in a timely manner after the inspection has been performed.

The current report documents pre-inspection predictions of temperatures for the two modules inspected at the Diablo Canyon ISFSI in January 2014. These are Module #318 (Cask 02-02) and Module #516 (Cask 03-05), which are site-specific variants of the HI-STORM 100A system. Site-specific data on the module design was not available prior to the inspection, so these predictions are based on the model of the overpack geometry developed for the inspections at the Hope Creek ISFSI (Cuta and Adkins, 2013). The model geometry for the Hope Creek site represents the HI-STORM 100S-218 Version B overpack, as documented in the HI-STORM100 FSAR. The canister portion of the model developed for the Diablo Canyon inspections is a generic MPC-32, which is reported to be somewhat different from the site-specific canisters used at the Diablo Canyon ISFSI.

These pre-inspection temperature predictions were obtained with detailed COBRA-SFS models of the two storage systems, as approximated with the available information, with the following boundary conditions and assumptions.

- storage module overpack configuration based on FSAR documentation of HI-STORM100S-218, Version B and standard MPC-32 canister; due to unavailability of site-specific design data for Diablo Canyon ISFSI modules
- Individual assembly and total decay heat loadings for each canister, based on at-loading values provided by PGE, “aged” to time of inspection using ORIGEN modeling
    - Special Note: there is an inherent conservatism of unquantified magnitude – informally estimated as approximately 20% -- in the utility-supplied values for at-loading assembly decay heat values
- Axial decay heat distributions based on a bounding generic profile for PWR fuel.
- Axial location of beginning of fuel assumed same as WE 17x17 OFA fuel, due to unavailability of specific data for WE17x17 STD and WE 17x17 Vantage 5 fuel designs
- Ambient conditions of still air at 50°F (10°C) assumed for base-case evaluations
    - Wind conditions at the Diablo Canyon site are unquantified, due to unavailability of site meteorological data
    - additional still-air evaluations performed at 70°F (21°C), 60°F (16°C), and 40°F (4°C), to cover a range of possible conditions at the time of the inspection. (Calculations were also performed at 80°F (27°C), for comparison with design basis assumptions.)

All calculations are for steady-state conditions, on the assumption that the surfaces of the module that are accessible for temperature measurements during the inspection will tend to follow ambient temperature changes relatively closely.

5.0 REFERENCES

10 CFR 71. 2003. "Packaging and Transportation of Radioactive Material." C*ode of Federal Regulations*, U.S. Nuclear Regulatory Commission, Washington D.C.

Creer JM, TE Michener, MA McKinnon, JE Tanner, ER Gilbert, and RL Goodman. 1987. *The TN-24P PWR Spent-Fuel Storage Cask: Testing and Analysis*. EPRI-NP-5128/PNL-6054, Electric Power Research Institute, Palo Alto, California.

Cuta JM and HE Adkins. 2013. Preliminary Thermal Modeling of HI-STORM100S-218 Version B Storage Modules at Hope Creek Nuclear Power Station ISFSI. FCRD-UFD-2013-000297, PNNL-22552. U.S. Department of Energy, Used Fuel Disposition Campaign, Washington, D.C.

DOE 1998. *Topical Report on Actinide-Only Burnup Credit for PWR Spent Nuclear Fuel Packages*. DOE/RW-0472, Revision 2, Office of Civilian Radioactive Waste Management, Washington D.C.

Holtec International, February 13, 2010. *Final Safety Analysis Report for the HI-STORM 100 Cask System, Revision 9.* Holtec Report No. HI-2002444, USNRC Docket No. 72-1014. Holtec International, Marlton, NJ. NOTE: this document is copyrighted intellectual property of Holtec International. All rights reserved.

Lombardo NJ, JM Cuta, TE Michener, DR Rector, and CL Wheeler. 1986. *COBRA-SFS: A Thermal-Hydraulic Analysis Computer Code, Volume III: Validation Assessments*. PNL-6048 Vol. III. Pacific Northwest Laboratory, Richland, Washington.

Michener TE, DR Rector, JM Cuta, RE Dodge, and CW Enderlin. 1995. *COBRA-SFS: A Thermal-Hydraulic Code for Spent Fuel Storage and Transportation Casks*. PNL-10782, Pacific Northwest Laboratory, Richland, Washington.

NOAA 2013. " National Weather Service Forecast Office, Los Angeles/Oxnard." Data for San Luis Obispo, CA, accessed 11/12/2013 at http://www.wrh.noaa.gov/yeardisp.php?stn=KSBP&wfo=lox&year=2012&span=Calendar+Year

Peterson J, et al. 2013. *Used Nuclear Fuel Storage Transportation Disposal Analysis Resources and Data System (UNF-ST&DARDS)*. FCRD-NFST-2013-000117 Rev. 0, Oak Ridge National Laboratory, Oak Ridge, Tennessee.

Rector DR, RA McCann, UP Jenquin, CM Heeb, JM Creer, and CL Wheeler. 1986. *CASTOR-1C Spent Fuel Storage Cask Decay Heat, Heat Transfer and Shielding Analysis*. PNL-5974. Pacific Northwest Laboratory, Richland, Washington.

Sparrow EM, and LFA Azevedo. 1985. "Vertical-channel natural convection spanning between the fully-developed limit and the single-plate boundary-layer limit." I*nternational Journal of Heat and Mass Transfer*, 28(10):1847-1857.

Sparrow EM, AL Loeffler, and HA Hubbard. 1961. "Heat Transfer to Longitudinal Laminar Flow between Cylinders." *Journal of Heat Transfer*, 83:415.

Suffield SR, JM Cuta, JA Fort, BA Collins, HE Adkins, and ER Siciliano. 2012. *Thermal Modeling of NUHOMS HSM-15 and HSM-1 Storage Modules at Calvert Cliffs Nuclear Power Station ISFSI.* PNNL-21788, Pacific Northwest National Laboratory, Richland, Washington.

Appendix A

Pre-Inspection Predictions of Axial Temperature Distribution on Canister Shell

Appendix A: Pre-Inspection Predictions of Axial Temperature Distribution on Canister Shell

This appendix presents the axial temperature distributions on the MPC outer shell predicted with the COBRA-SFS models of Modules #318 (02-02) and #516 (03-05) in the Diablo Canyon ISFSI. These profiles are through the location of the peak temperature on the MPC outer shell for each configuration. A second profile is provided for the peak temperature in the cooler regions opposite the MPC-32 basket corners, showing the circumferential variation in canister shell temperature predicted for this storage system. The axial location in the tables is relative to the inner surface of the canister base. Results are presented for each of the two canisters in Tables A-1 and A-2, at the reference ambient temperature of 50°F (10°C). Tables A-5 and A-6 present results for a range of ambient conditions, postulated to span the most likely range for ambient temperature at the time of the inspection, originally scheduled for early December 2013, and actually accomplished in January 2014.

Table A-1. Canister Shell Axial Temperature Distribution: Module #318 (02-02) (50°F (10°C Ambient)

Ambient:	**50**	**(°F)**	**10**	**(°C)**
axial location	**peak profile**		**profile over basket corner**	
(inches)	**(°F)**	**(°C)**	**(°F)**	**(°C)**
4.1	135.81	57.67	116.59	46.99
8.1	130.50	54.72	102.60	39.22
12.2	129.78	54.32	98.07	36.70
16.2	130.89	54.94	97.44	36.36
20.3	132.78	55.99	98.45	36.91
24.3	134.99	57.22	100.13	37.85
28.4	137.34	58.52	102.09	38.94
32.4	139.74	59.85	104.16	40.09
36.5	142.14	61.19	106.27	41.26
40.5	144.54	62.52	108.40	42.44
44.6	146.93	63.85	110.53	43.63
48.6	149.31	65.17	112.65	44.81
52.7	151.68	66.49	114.77	45.99
56.7	154.03	67.80	116.89	47.16
60.8	156.39	69.10	119.01	48.34
64.8	158.74	70.41	121.13	49.52
68.9	161.08	71.71	123.26	50.70
72.9	163.43	73.02	125.38	51.88
77	165.78	74.32	127.51	53.06
81	168.14	75.63	129.65	54.25
85.1	170.50	76.94	131.80	55.45
89.2	172.86	78.26	133.96	56.64
93.2	175.24	79.58	136.12	57.85

97.3	177.62	80.90	138.30	59.05
101.3	180.01	82.23	140.48	60.27
105.4	182.41	83.56	142.67	61.49
109.4	184.82	84.90	144.87	62.71
113.5	187.23	86.24	147.07	63.93
117.5	189.64	87.58	149.27	65.15
121.6	192.05	88.91	151.46	66.36
125.6	194.44	90.24	153.61	67.56
129.7	196.80	91.56	155.72	68.73
133.7	199.12	92.84	157.75	69.86
137.8	201.37	94.09	159.67	70.93
141.8	203.55	95.31	161.47	71.93
145.9	205.68	96.49	163.17	72.87
149.9	207.79	97.66	164.79	73.77
154	209.96	98.87	166.45	74.70
158	212.27	100.15	168.30	75.72
162.1	214.81	101.56	170.52	76.96
166.1	217.71	103.17	173.51	78.62
170.2	221.29	105.16	178.28	81.26
174.2	226.41	108.00	187.40	86.33
178.3	235.44	113.02	207.56	97.53

Table A-2. Canister Shell Axial Temperature Distribution: Module #516 (03-05) (50°F (10°C Ambient)

Ambient:	**50**	**(°F)**	**10**	**(°C)**
axial location	**peak profile**		**profile over basket corner**	
(inches)	**(°F)**	**(°C)**	**(°F)**	**(°C)**
4.1	122.07	50.04	105.87	41.04
8.1	117.61	47.56	94.01	34.45
12.2	116.98	47.21	90.08	32.27
16.2	117.91	47.73	89.46	31.92
20.3	119.49	48.60	90.21	32.34
24.3	121.34	49.63	91.55	33.08
28.4	123.31	50.73	93.12	33.95
32.4	125.32	51.84	94.79	34.88
36.5	127.34	52.97	96.50	35.83
40.5	129.36	54.09	98.22	36.79
44.6	131.37	55.21	99.96	37.75
48.6	133.38	56.32	101.69	38.72
52.7	135.38	57.43	103.42	39.68
56.7	137.37	58.54	105.16	40.64
60.8	139.36	59.65	106.89	41.61
64.8	141.35	60.75	108.63	42.57

68.9	143.34	61.86	110.38	43.54
72.9	145.33	62.96	112.13	44.51
77	147.33	64.07	113.88	45.49
81	149.33	65.18	115.65	46.47
85.1	151.33	66.30	117.42	47.45
89.2	153.34	67.41	119.20	48.44
93.2	155.36	68.54	120.99	49.44
97.3	157.39	69.66	122.79	50.44
101.3	159.43	70.79	124.60	51.44
105.4	161.47	71.93	126.42	52.45
109.4	163.52	73.07	128.24	53.47
113.5	165.58	74.21	130.07	54.48
117.5	167.64	75.36	131.90	55.50
121.6	169.70	76.50	133.72	56.51
125.6	171.75	77.64	135.52	57.51
129.7	173.77	78.76	137.29	58.49
133.7	175.76	79.87	139.00	59.45
137.8	177.70	80.94	140.65	60.36
141.8	179.59	81.99	142.21	61.23
145.9	181.44	83.02	143.71	62.06
149.9	183.29	84.05	145.18	62.88
154	185.18	85.10	146.70	63.72
158	187.20	86.22	148.38	64.66
162.1	189.42	87.45	150.39	65.77
166.1	191.95	88.86	153.09	67.27
170.2	195.07	90.59	157.35	69.64
174.2	199.49	93.05	165.44	74.13
178.3	207.22	97.35	183.02	83.90

Table A-3. Peak Canister Shell Axial Temperature Distributions over Basket 'Corner' for Module #318 (02-02) for a Range of Ambient Temperatures

axial location (inches)	Module #318 (02-02) (17.05 kW as of December 2013)							
	80°F (27°C) ambient		70°F (21°C) ambient		60°F (16°C) ambient		40°F (4.4°C) ambient	
	(°F)	(°C)	(°F)	(°C)	(°F)	(°C)	(°F)	(°C)
4.1	145.24	62.91	135.73	57.63	126.19	52.33	107.12	41.73
8.1	132.66	55.92	122.68	50.38	112.68	44.82	92.66	33.70
12.2	128.82	53.79	118.62	48.12	108.39	42.44	87.91	31.06
16.2	128.59	53.66	118.26	47.92	107.90	42.17	87.16	30.65
20.3	129.85	54.36	119.44	48.58	109.00	42.78	88.09	31.16
24.3	131.74	55.41	121.27	49.59	110.77	43.76	89.72	32.06
28.4	133.88	56.60	123.35	50.75	112.79	44.89	91.62	33.12
32.4	136.11	57.84	125.53	51.96	114.92	46.07	93.64	34.24
36.5	138.37	59.09	127.74	53.19	117.09	47.27	95.69	35.38

40.5	140.63	60.35	129.96	54.42	119.27	48.48	97.75	36.53
44.6	142.89	61.61	132.18	55.66	121.44	49.69	99.82	37.68
48.6	145.15	62.86	134.39	56.88	123.61	50.90	101.89	38.83
52.7	147.40	64.11	136.60	58.11	125.78	52.10	103.95	39.97
56.7	149.64	65.36	138.81	59.34	127.94	53.30	106.02	41.12
60.8	151.88	66.60	141.01	60.56	130.11	54.50	108.09	42.27
64.8	154.12	67.85	143.21	61.78	132.27	55.71	110.17	43.43
68.9	156.36	69.09	145.42	63.01	134.44	56.91	112.25	44.59
72.9	158.61	70.34	147.62	64.24	136.60	58.11	114.34	45.74
77	160.86	71.59	149.84	65.46	138.78	59.32	116.43	46.91
81	163.12	72.84	152.06	66.70	140.96	60.53	118.54	48.08
85.1	165.39	74.10	154.29	67.94	143.15	61.75	120.65	49.25
89.2	167.66	75.37	156.52	69.18	145.35	62.97	122.76	50.42
93.2	169.94	76.64	158.77	70.43	147.56	64.20	124.89	51.61
97.3	172.24	77.91	161.02	71.68	149.78	65.43	127.03	52.79
101.3	174.54	79.19	163.29	72.94	152.00	66.67	129.17	53.98
105.4	176.85	80.47	165.56	74.20	154.24	67.91	131.32	55.18
109.4	179.16	81.76	167.84	75.47	156.48	69.15	133.48	56.38
113.5	181.48	83.05	170.12	76.73	158.72	70.40	135.65	57.58
117.5	183.79	84.33	172.40	78.00	160.96	71.64	137.81	58.78
121.6	186.09	85.61	174.66	79.25	163.18	72.88	139.95	59.97
125.6	188.35	86.86	176.89	80.49	165.38	74.10	142.08	61.15
129.7	190.56	88.09	179.06	81.70	167.52	75.29	144.15	62.31
133.7	192.67	89.26	181.15	82.86	169.58	76.43	146.15	63.42
137.8	194.66	90.37	183.11	83.95	171.53	77.51	148.05	64.47
141.8	196.51	91.40	184.95	84.97	173.35	78.53	149.84	65.47
145.9	198.24	92.36	186.67	85.93	175.05	79.47	151.52	66.40
149.9	199.89	93.27	188.32	86.84	176.69	80.39	153.14	67.30
154	201.59	94.21	190.00	87.78	178.37	81.31	154.79	68.21
158	203.48	95.27	191.88	88.82	180.23	82.35	156.62	69.23
162.1	205.75	96.53	194.13	90.07	182.47	83.59	158.82	70.46
166.1	208.78	98.21	197.15	91.75	185.47	85.26	161.80	72.11
170.2	213.52	100.84	201.90	94.39	190.23	87.91	166.58	74.77
174.2	222.44	105.80	210.89	99.38	199.29	92.94	175.77	79.87
178.3	242.01	116.67	230.65	110.36	219.25	104.03	196.15	91.19

Table A-4. Peak Canister Shell Axial Temperature Distributions over Basket 'Corner' for Module #516 (03-05) for a Range of Ambient Temperatures

axial location (inches)	Module #516 (03-05) (13.87 kW as of December 2013)							
	80°F (27°C) ambient		70°F (21°C) ambient		60°F (16°C) ambient		40°F (4.4°C) ambient	
	(°F)	(°C)	(°F)	(°C)	(°F)	(°C)	(°F)	(°C)
4.1	134.48	56.93	124.97	57.63	115.45	52.33	96.41	41.73
8.1	123.90	51.05	113.97	50.38	104.02	44.82	84.12	33.70
12.2	120.59	49.22	110.46	48.12	100.31	42.44	79.99	31.06
16.2	120.31	49.06	110.07	47.92	99.80	42.17	79.26	30.65

20.3	121.29	49.61	110.98	48.58	100.64	42.78	79.95	31.16
24.3	122.80	50.44	112.43	49.59	102.04	43.76	81.24	32.06
28.4	124.52	51.40	114.11	50.75	103.67	44.89	82.77	33.12
32.4	126.32	52.40	115.87	51.96	105.40	46.07	84.40	34.24
36.5	128.15	53.42	117.66	53.19	107.15	47.27	86.07	35.38
40.5	129.99	54.44	119.47	54.42	108.92	48.48	87.75	36.53
44.6	131.83	55.46	121.27	55.66	110.69	49.69	89.43	37.68
48.6	133.66	56.48	123.08	56.88	112.46	50.90	91.12	38.83
52.7	135.50	57.50	124.88	58.11	114.23	52.10	92.80	39.97
56.7	137.34	58.52	126.68	59.34	116.00	53.30	94.49	41.12
60.8	139.18	59.54	128.49	60.56	117.77	54.50	96.18	42.27
64.8	141.02	60.57	130.30	61.78	119.55	55.71	97.88	43.43
68.9	142.86	61.59	132.11	63.01	121.33	56.91	99.58	44.59
72.9	144.71	62.62	133.93	64.24	123.11	58.11	101.30	45.74
77	146.57	63.65	135.75	65.46	124.91	59.32	103.02	46.91
81	148.44	64.69	137.59	66.70	126.71	60.53	104.75	48.08
85.1	150.32	65.73	139.43	67.94	128.52	61.75	106.49	49.25
89.2	152.20	66.78	141.28	69.18	130.34	62.97	108.24	50.42
93.2	154.10	67.83	143.14	70.43	132.16	64.20	110.00	51.61
97.3	156.00	68.89	145.02	71.68	134.00	65.43	111.76	52.79
101.3	157.92	69.95	146.90	72.94	135.85	66.67	113.54	53.98
105.4	159.84	71.02	148.79	74.20	137.70	67.91	115.32	55.18
109.4	161.77	72.10	150.68	75.47	139.57	69.15	117.11	56.38
113.5	163.71	73.17	152.59	76.73	141.43	70.40	118.90	57.58
117.5	165.64	74.24	154.49	78.00	143.30	71.64	120.70	58.78
121.6	167.56	75.31	156.38	79.25	145.16	72.88	122.49	59.97
125.6	169.47	76.37	158.25	80.49	146.99	74.10	124.26	61.15
129.7	171.33	77.40	160.08	81.70	148.79	75.29	125.99	62.31
133.7	173.12	78.40	161.85	82.86	150.54	76.43	127.68	63.42
137.8	174.84	79.36	163.54	83.95	152.21	77.51	129.30	64.47
141.8	176.47	80.26	165.15	84.97	153.80	78.53	130.85	65.47
145.9	178.02	81.12	166.68	85.93	155.32	79.47	132.33	66.40
149.9	179.54	81.96	168.19	86.84	156.80	80.39	133.78	67.30
154	181.10	82.84	169.74	87.78	158.34	81.31	135.29	68.21
158	182.85	83.80	171.46	88.82	160.05	82.35	136.95	69.23
162.1	184.92	84.96	173.52	90.07	162.08	83.59	138.94	70.46
166.1	187.67	86.48	176.25	91.75	164.79	85.26	141.61	72.11
170.2	191.93	88.85	180.52	94.39	169.06	87.91	145.88	74.77
174.2	199.87	93.26	188.51	99.38	177.10	92.94	154.02	79.87
178.3	216.99	102.77	205.78	110.36	194.53	104.03	171.76	91.19

Table A-5. Peak Canister Shell Axial Temperature Distributions for Module #318 (02-02) for a Range of Ambient Temperatures

axial location (inches)	Module #318 (02-02) (17.05 kW as of December 2013)							
	80°F (27°C) ambient		70°F (21°C) ambient		60°F (16°C) ambient		40°F (4.4°C) ambient	
	(°F)	(°C)	(°F)	(°C)	(°F)	(°C)	(°F)	(°C)
4.1	163.26	72.92	154.16	67.86	145.02	62.79	126.76	52.64
8.1	158.75	70.42	149.38	65.21	139.99	59.99	121.18	49.54
12.2	158.43	70.24	148.94	64.96	139.41	59.67	120.33	49.07
16.2	159.80	71.00	150.23	65.68	140.63	60.35	121.38	49.65
20.3	161.88	72.15	152.24	66.80	142.59	61.44	123.21	50.67
24.3	164.25	73.47	154.57	68.09	144.86	62.70	125.39	51.88
28.4	166.73	74.85	157.01	69.45	147.27	64.04	127.69	53.16
32.4	169.26	76.25	159.50	70.83	149.71	65.39	130.03	54.46
36.5	171.78	77.65	161.98	72.21	152.16	66.75	132.38	55.77
40.5	174.29	79.05	164.46	73.59	154.60	68.11	134.73	57.07
44.6	176.79	80.44	166.92	74.96	157.03	69.46	137.07	58.37
48.6	179.27	81.82	169.37	76.32	159.44	70.80	139.39	59.66
52.7	181.74	83.19	171.81	77.67	161.85	72.14	141.71	60.95
56.7	184.20	84.56	174.24	79.02	164.24	73.47	144.02	62.23
60.8	186.65	85.92	176.66	80.37	166.63	74.79	146.34	63.52
64.8	189.10	87.28	179.07	81.71	169.01	76.12	148.65	64.81
68.9	191.54	88.63	181.49	83.05	171.40	77.44	150.96	66.09
72.9	193.99	89.99	183.90	84.39	173.78	78.77	153.28	67.38
77	196.43	91.35	186.32	85.73	176.16	80.09	155.60	68.67
81	198.89	92.71	188.74	87.08	178.55	81.42	157.92	69.96
85.1	201.34	94.08	191.16	88.42	180.95	82.75	160.25	71.25
89.2	203.80	95.45	193.60	89.78	183.35	84.08	162.58	72.55
93.2	206.27	96.82	196.04	91.13	185.76	85.42	164.92	73.85
97.3	208.75	98.20	198.48	92.49	188.18	86.76	167.27	75.15
101.3	211.24	99.58	200.94	93.86	190.60	88.11	169.63	76.46
105.4	213.74	100.97	203.41	95.23	193.04	89.46	172.00	77.78
109.4	216.24	102.36	205.88	96.60	195.48	90.82	174.37	79.09
113.5	218.75	103.75	208.36	97.98	197.92	92.18	176.75	80.42
117.5	221.26	105.15	210.84	99.36	200.37	93.54	179.13	81.74
121.6	223.77	106.54	213.32	100.73	202.82	94.90	181.50	83.06
125.6	226.26	107.92	215.78	102.10	205.24	96.25	183.86	84.37
129.7	228.72	109.29	218.20	103.45	207.64	97.58	186.19	85.66
133.7	231.13	110.63	220.58	104.77	209.99	98.88	188.47	86.93
137.8	233.47	111.93	222.90	106.05	212.27	100.15	190.69	88.16
141.8	235.75	113.19	225.14	107.30	214.49	101.38	192.85	89.36
145.9	237.96	114.42	227.33	108.52	216.65	102.58	194.95	90.53
149.9	240.17	115.65	229.51	109.73	218.80	103.78	197.03	91.68
154	242.44	116.91	231.75	110.97	221.00	105.00	199.16	92.87
158	244.87	118.26	234.14	112.30	223.35	106.31	201.44	94.13
162.1	247.54	119.75	236.77	113.76	225.94	107.74	203.93	95.52
166.1	250.58	121.43	239.76	115.42	228.88	109.38	206.78	97.10

170.2	254.30	123.50	243.43	117.46	232.51	111.40	210.33	99.07
174.2	259.50	126.39	248.60	120.34	237.65	114.25	215.42	101.90
178.3	268.55	131.42	257.64	125.36	246.69	119.27	224.47	106.93

Table A-6. Peak Canister Shell Axial Temperature Distributions for Module #516 (03-05) for a Range of Ambient Temperatures

axial location (inches)	Module #516 (03-05) (13.87 kW as of December 2013)							
	80°F (27°C) ambient		70°F (21°C) ambient		60°F (16°C) ambient		40°F (4.4°C) ambient	
	(°F)	(°C)	(°F)	(°C)	(°F)	(°C)	(°F)	(°C)
4.1	149.65	65.36	140.49	60.27	131.32	55.18	112.97	44.98
8.1	145.94	63.30	136.53	58.07	127.11	52.84	108.26	42.37
12.2	145.69	63.16	136.16	57.87	126.62	52.57	107.52	41.95
16.2	146.84	63.80	137.25	58.47	127.63	53.13	108.37	42.43
20.3	148.59	64.77	138.94	59.41	129.27	54.04	109.90	43.28
24.3	150.58	65.88	140.89	60.50	131.18	55.10	111.72	44.29
28.4	152.67	67.04	142.95	61.64	133.20	56.22	113.66	45.36
32.4	154.79	68.22	145.04	62.80	135.26	57.37	115.63	46.46
36.5	156.92	69.40	147.13	63.96	137.32	58.51	117.61	47.56
40.5	159.04	70.58	149.22	65.12	139.38	59.65	119.59	48.66
44.6	161.14	71.75	151.30	66.28	141.43	60.79	121.56	49.75
48.6	163.24	72.91	153.37	67.43	143.47	61.93	123.52	50.85
52.7	165.33	74.07	155.43	68.57	145.50	63.05	125.48	51.93
56.7	167.41	75.23	157.48	69.71	147.52	64.18	127.43	53.02
60.8	169.49	76.38	159.53	70.85	149.54	65.30	129.38	54.10
64.8	171.57	77.54	161.58	71.99	151.56	66.42	131.33	55.18
68.9	173.64	78.69	163.63	73.13	153.58	67.55	133.28	56.27
72.9	175.72	79.84	165.68	74.26	155.60	68.67	135.24	57.36
77	177.80	81.00	167.73	75.41	157.63	69.79	137.21	58.45
81	179.89	82.16	169.79	76.55	159.66	70.92	139.18	59.54
85.1	181.98	83.32	171.85	77.70	161.70	72.05	141.15	60.64
89.2	184.08	84.49	173.93	78.85	163.74	73.19	143.14	61.74
93.2	186.19	85.66	176.01	80.00	165.79	74.33	145.13	62.85
97.3	188.31	86.84	178.10	81.16	167.85	75.47	147.12	63.96
101.3	190.43	88.02	180.20	82.33	169.92	76.62	149.13	65.07
105.4	192.57	89.21	182.30	83.50	172.00	77.78	151.14	66.19
109.4	194.71	90.40	184.42	84.68	174.08	78.94	153.16	67.31
113.5	196.87	91.59	186.54	85.85	176.18	80.10	155.19	68.44
117.5	199.02	92.79	188.66	87.04	178.27	81.26	157.22	69.57
121.6	201.17	93.98	190.79	88.21	180.36	82.42	159.25	70.69
125.6	203.31	95.17	192.90	89.39	182.44	83.58	161.26	71.81
129.7	205.43	96.35	194.98	90.55	184.50	84.72	163.25	72.92
133.7	207.51	97.51	197.04	91.69	186.52	85.84	165.21	74.01
137.8	209.54	98.63	199.04	92.80	188.49	86.94	167.12	75.07
141.8	211.52	99.74	200.99	93.88	190.41	88.01	168.98	76.10

145.9	213.47	100.81	202.90	94.95	192.30	89.05	170.80	77.11
149.9	215.41	101.89	204.82	96.01	194.18	90.10	172.62	78.12
154	217.41	103.01	206.78	97.10	196.11	91.17	174.48	79.15
158	219.55	104.20	208.88	98.27	198.17	92.32	176.46	80.26
162.1	221.90	105.50	211.19	99.55	200.43	93.57	178.63	81.46
166.1	224.56	106.98	213.81	101.00	203.01	95.00	181.12	82.84
170.2	227.81	108.78	217.01	102.78	206.17	96.76	184.20	84.55
174.2	232.33	111.29	221.50	105.28	210.63	99.24	188.59	87.00
178.3	240.10	115.61	229.25	109.58	218.37	103.54	196.32	91.29